EPFL

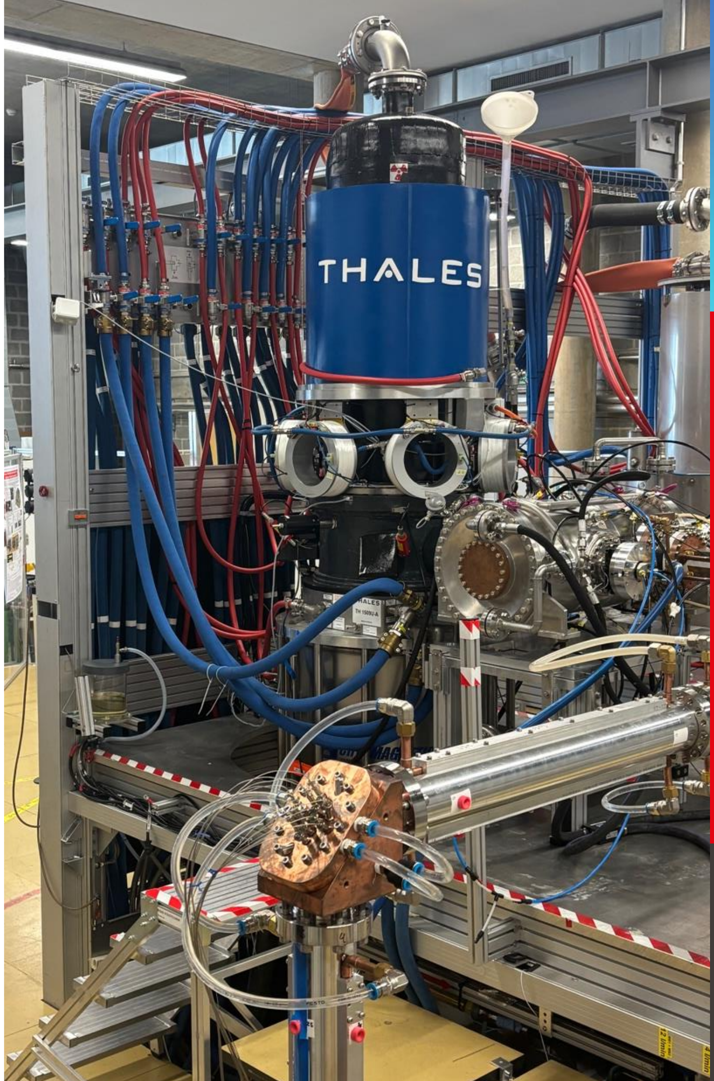

IIS2026

ITER International School

Physics and engineering of heating and current drive systems for magnetic fusion plasmas

(L-2) EC principles: technology overview

Jeremy Genoud

乐山

20.07.2026

Swiss
Plasma
Center

ITER external heating systems

- ITER has plans for EC, NBI and IC
  - NBI: heating, current drive, fueling, rotation
  - IC:heating, wall conditioning, impurity control
  - EC: start-up, heating, current-drive, instability mitigation/control, impurity control

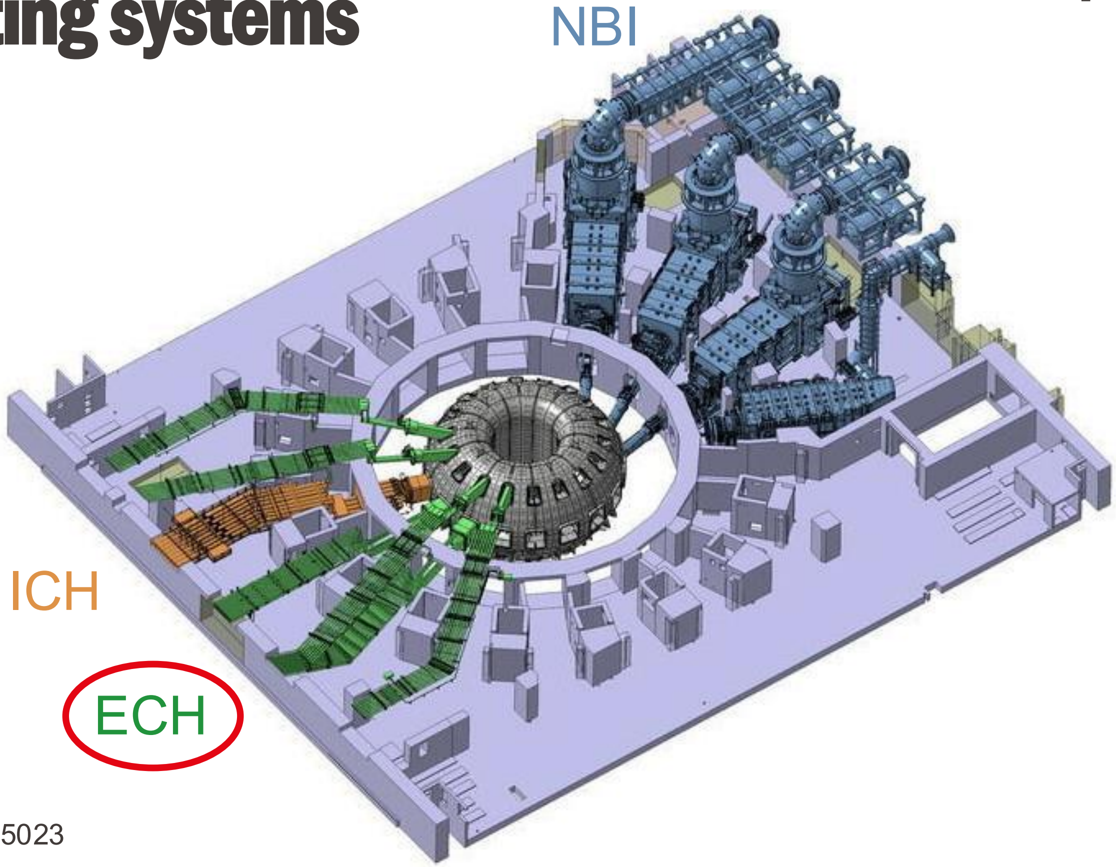

A Loarte et al 2025 Plasma Phys. Control. Fusion 67 065023

https://www.iter.org/machine/supporting-systems/external-heating-systems

ITER external heating systems

Outline

- 1. Sources
- 2. Transmission lines and components
- 3. Launchers

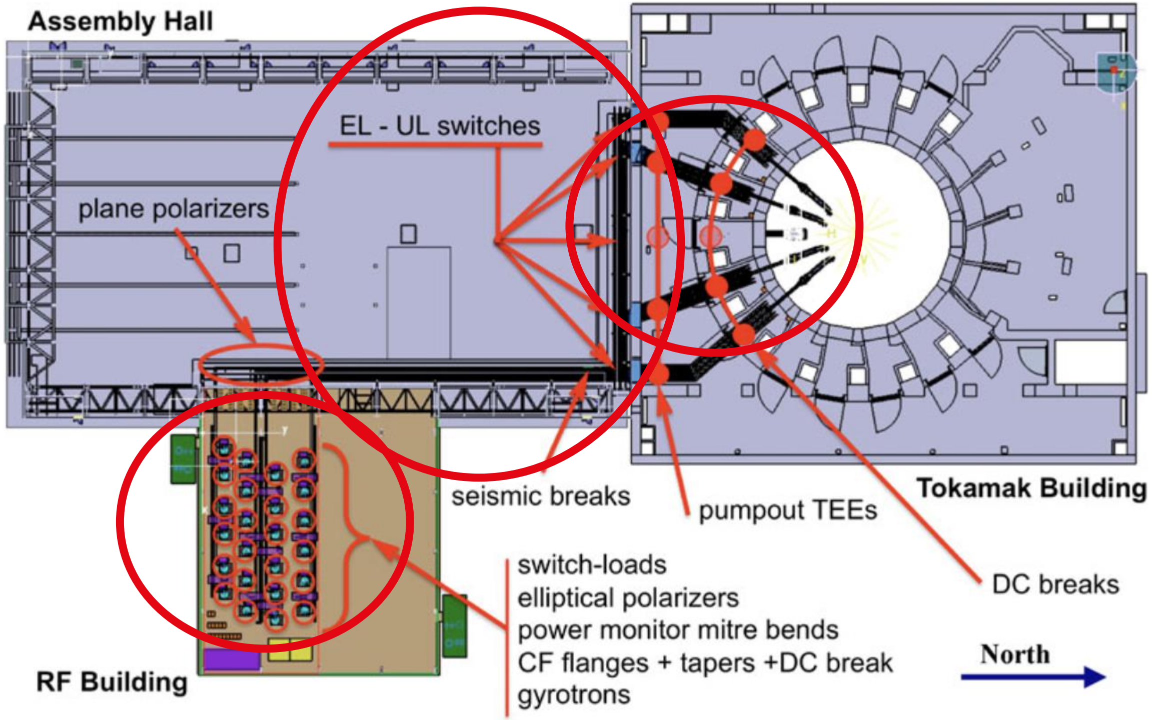

F. Gandini, Fusion Science and Technology (2010)

ITER external heating systems

<u>Outline</u>

- 1. Sources
- 2. Transmission lines and components
- 3. Launchers

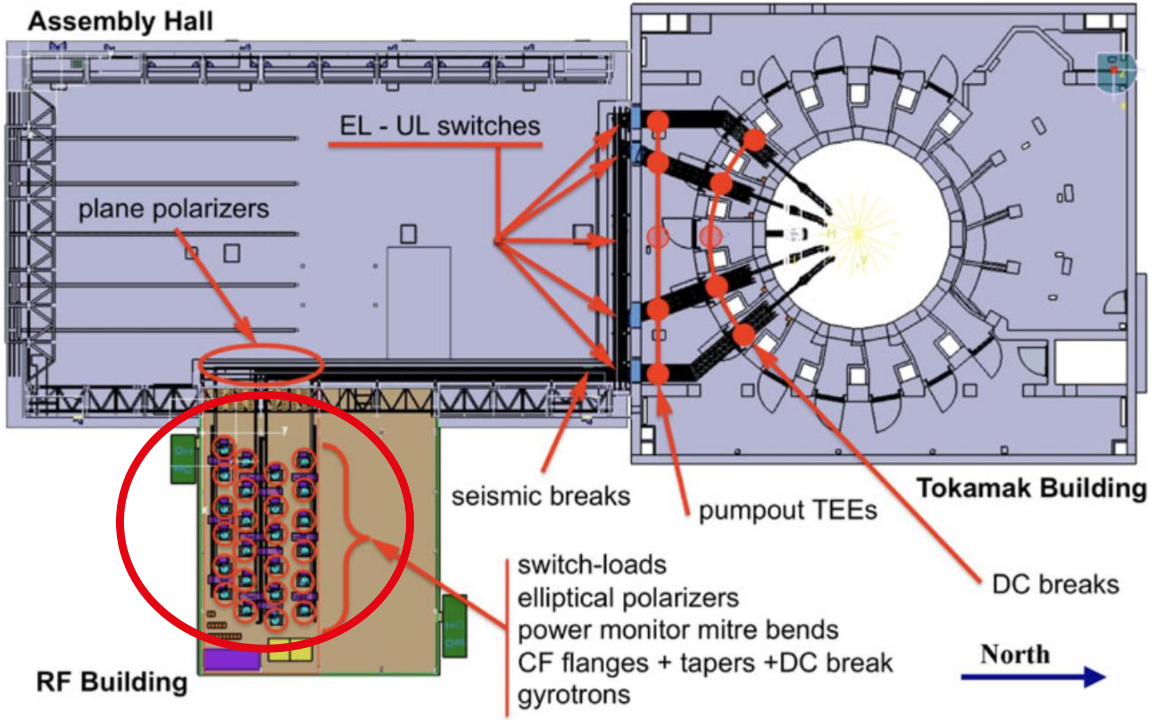

F. Gandini, Fusion Science and Technology (2010)

1. The source: The gyrotron

- High-power gyrotrons (ECRH, ECCD)
  - f ~ 80-170 GHz*
  - P ~ 1 MW*

  *DEMO (200GHz, 2MW ?)
- Low-power gyrotrons (DNP-NMR spectroscopy)
  - f ~ 260 GHz
  - P ~ 100 W

The THz Gap

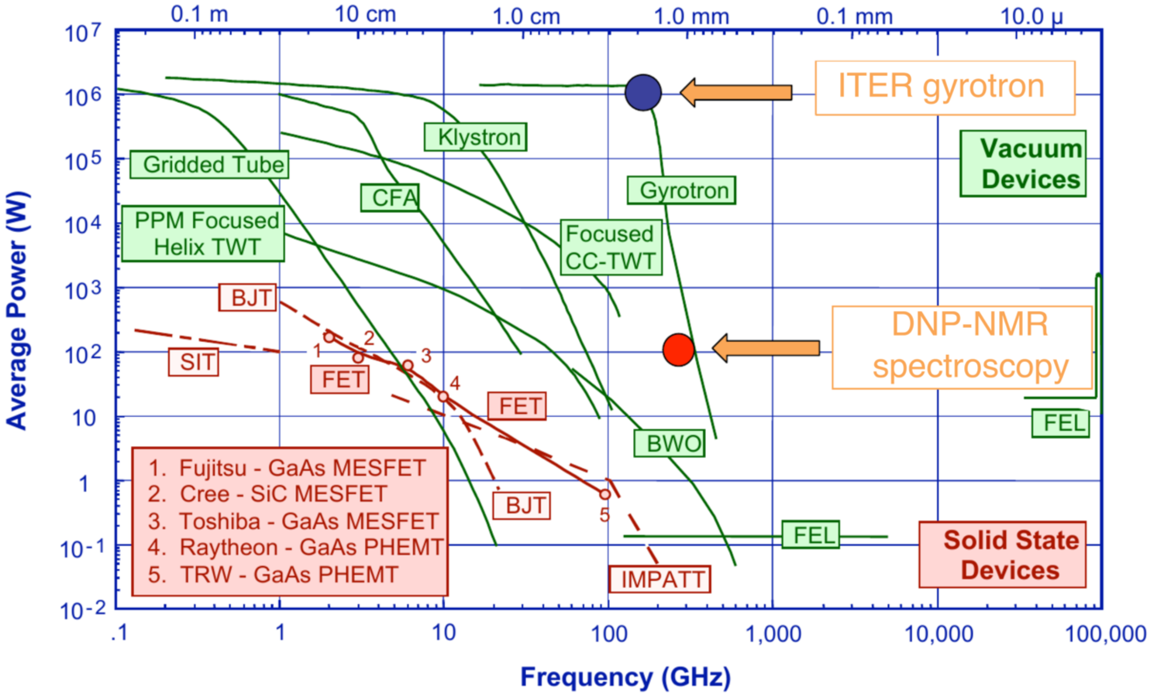

Colin Joye, MIT, 2004

The gyrotron for ITER (EU-DA version)

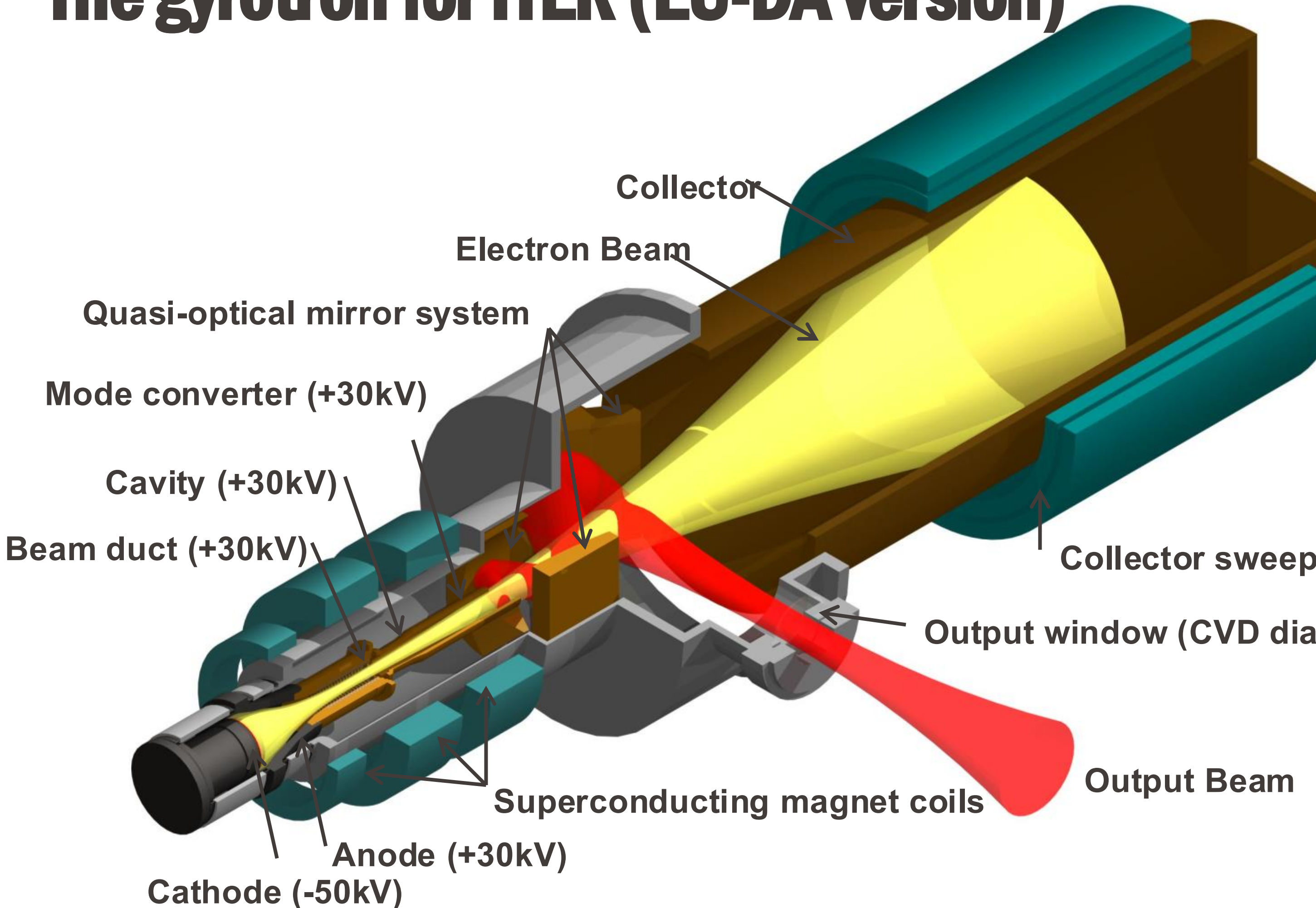

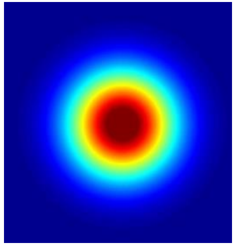

Swiss Plasma Center

Key Elements of the Interaction

- Generate coherent Electromagnetic radiation by stimulated emission from a beam of relativistic electrons.

- Magnetized electron beam
  - $\Omega_c = \frac{e\,B_0}{m_0}$

- High kinetic energy
  - $\gamma = 1 + \frac{e\mathrm{V_b}}{m_0 c^2}$
  - $\widetilde{\Omega}_\mathrm{c} = \frac{\Omega_c}{\gamma}$

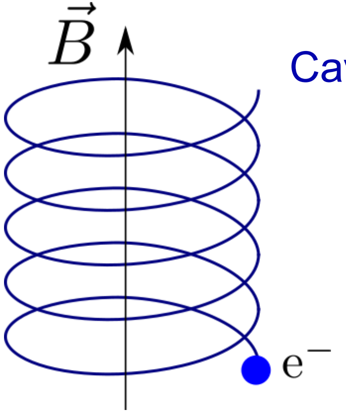

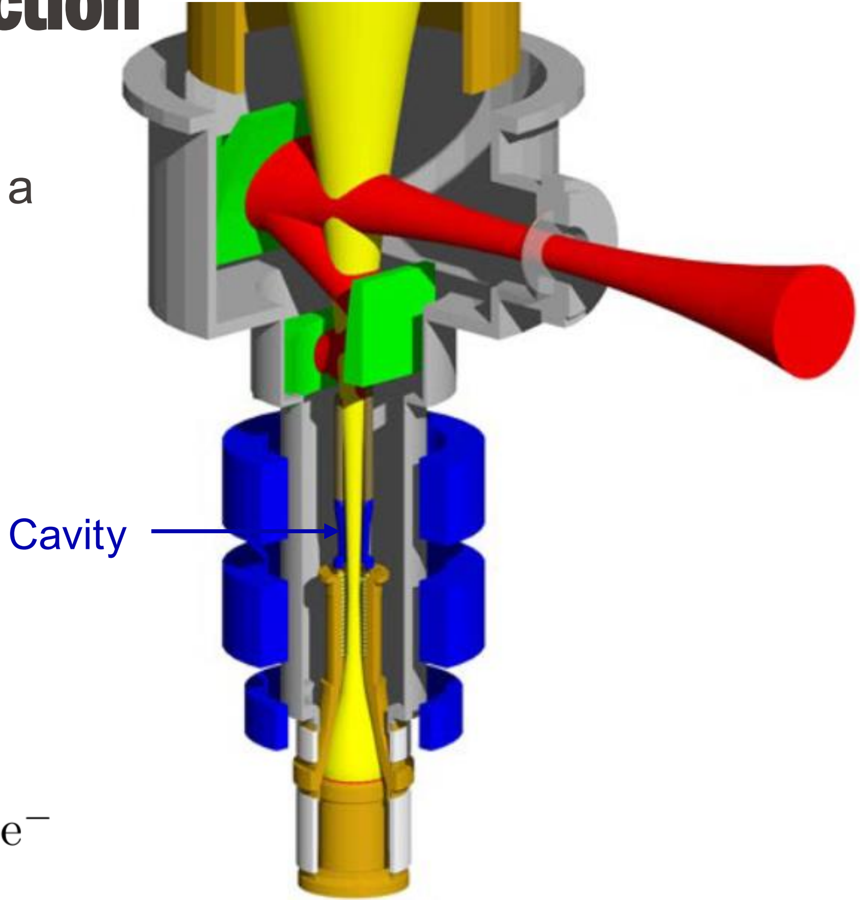

Key Elements of the Interaction: e- beam

- Electron trajectory:
  - Guiding center radius

$$|\vec{r_g}| = R_b = r_{\text{cath}}\sqrt{\frac{B_{cath}}{B_{\text{cav}}}}$$

  - Larmor radius (gyromotion)

$$r_L = \frac{mv_\perp}{|q|B}$$

  - $|\vec{r_L}| \ll |\vec{r_g}| = R_b$

- Electron beam dispersion relation

$$\omega_b = s\frac{\Omega_c}{\gamma} + k_\parallel v_\parallel$$

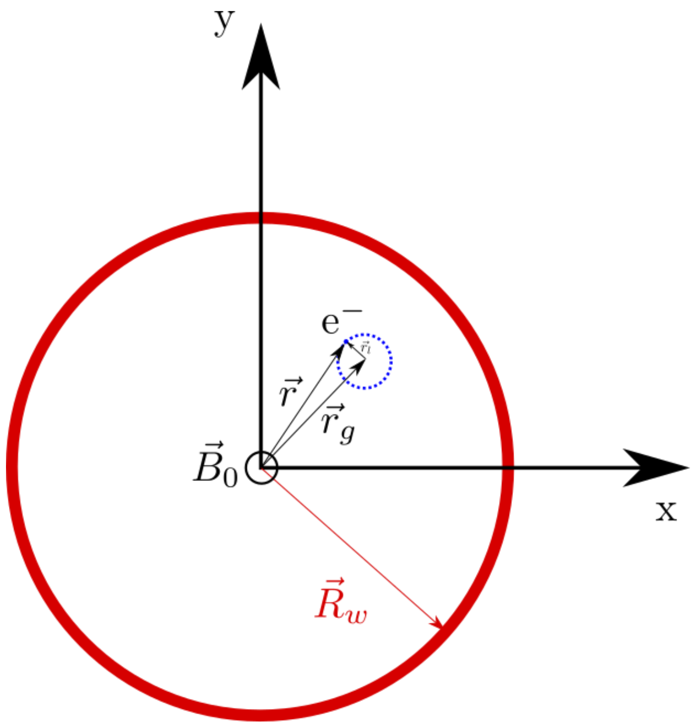

Key Elements of the Interaction: EM wave in cavity

- Electromagnetic wave supported by the cavity (TE-modes in cylindrical cavity)

- Dispersion relation

$$\omega_{\mathrm{m,p},q} = c\sqrt{k_\perp^2 + k_\parallel^2}$$

$$k_\perp = \frac{\nu_{m,p}}{R}$$

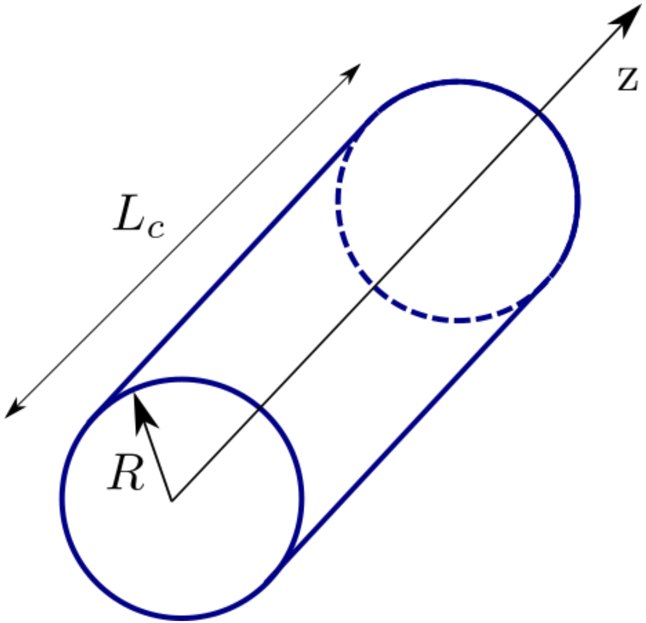

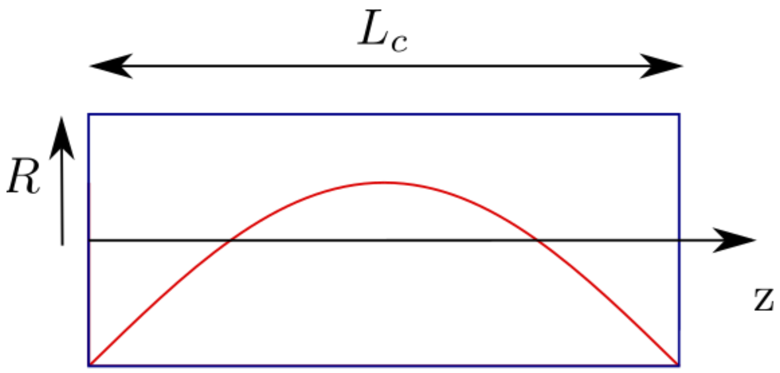

For a finite length cavity with perfectly conducting B.C.

$$k_\parallel = q\frac{\pi}{L_c}$$

$k_\parallel \ll k_\perp \Rightarrow$ R fixes the frequency

Key Elements of the Interaction: EM wave in cavity

- Electromagnetic wave supported by the cavity $TE_{m,p,q}$
  - Longitudinal profile (high-power -> q=1)

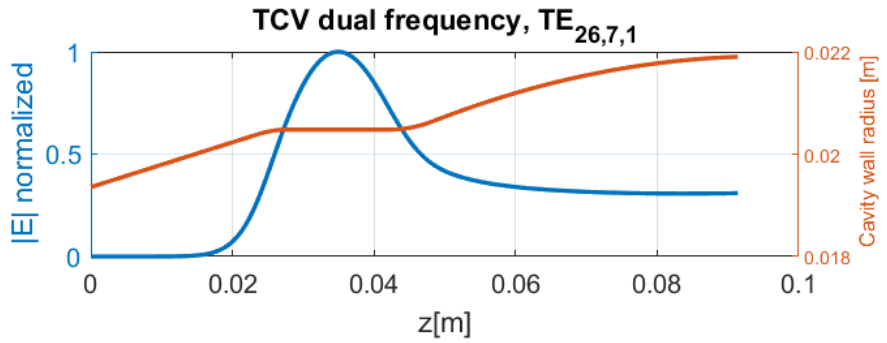

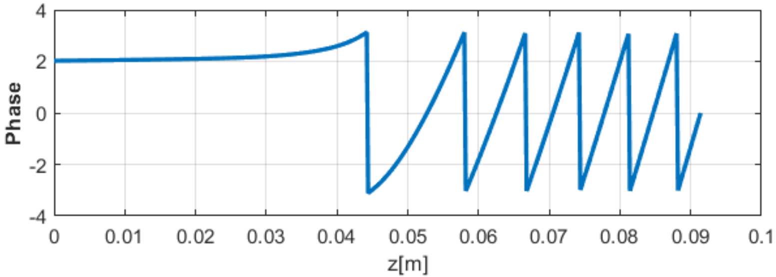

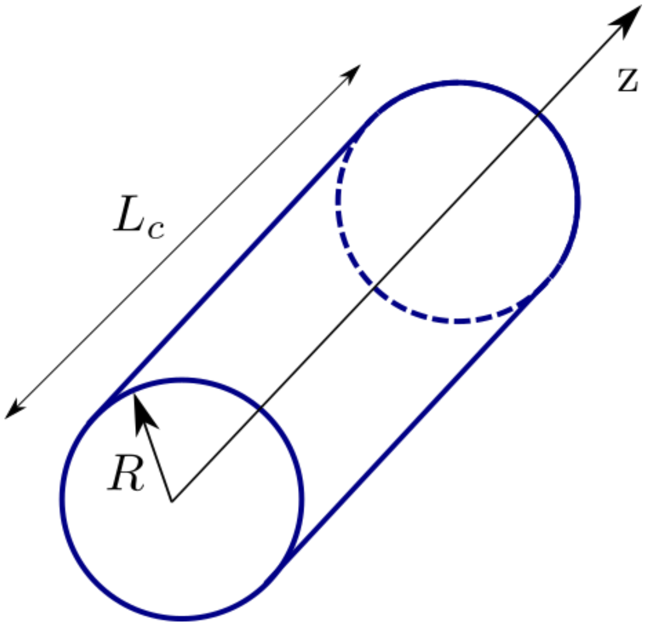

Key Elements of the Interaction: EM wave in cavity

- Electromagnetic wave supported by the cavity $TE_{m,p,q}$
  - Longitudinal profile (high-power -> q=1)
  - Transverse profile (m,p)

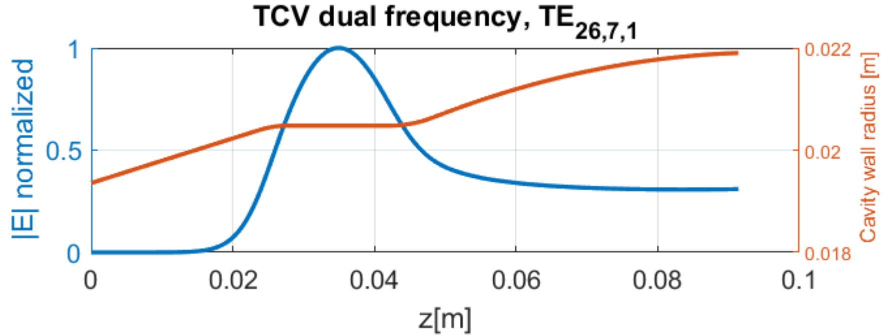

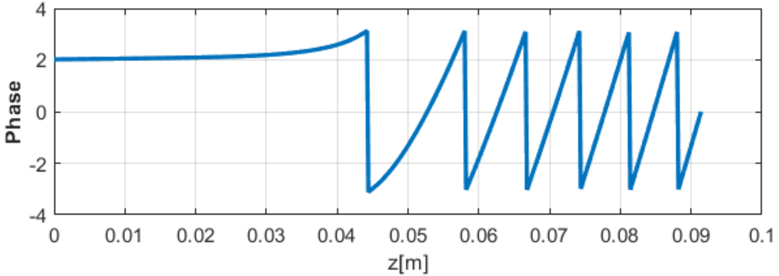

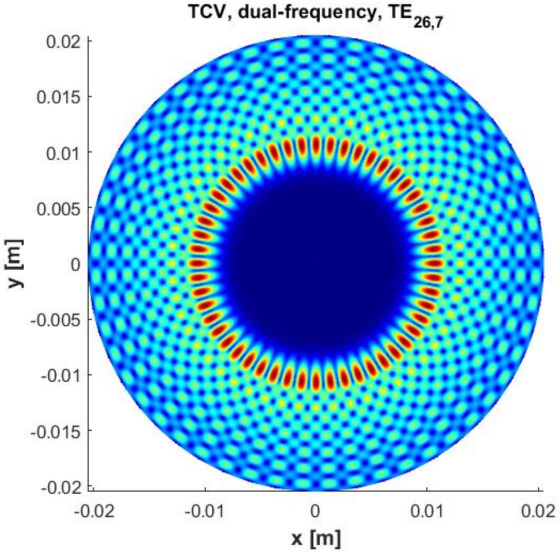

Magnetic Field Alignment

- The cavity has a **mechanical axis** defined by the gyrotron construction
- The **magnetic axis** is defined by the SC-system
- The magnetic and mechanical axes need to be aligned at very high precision ($|\delta r| < 0.1$ mm)

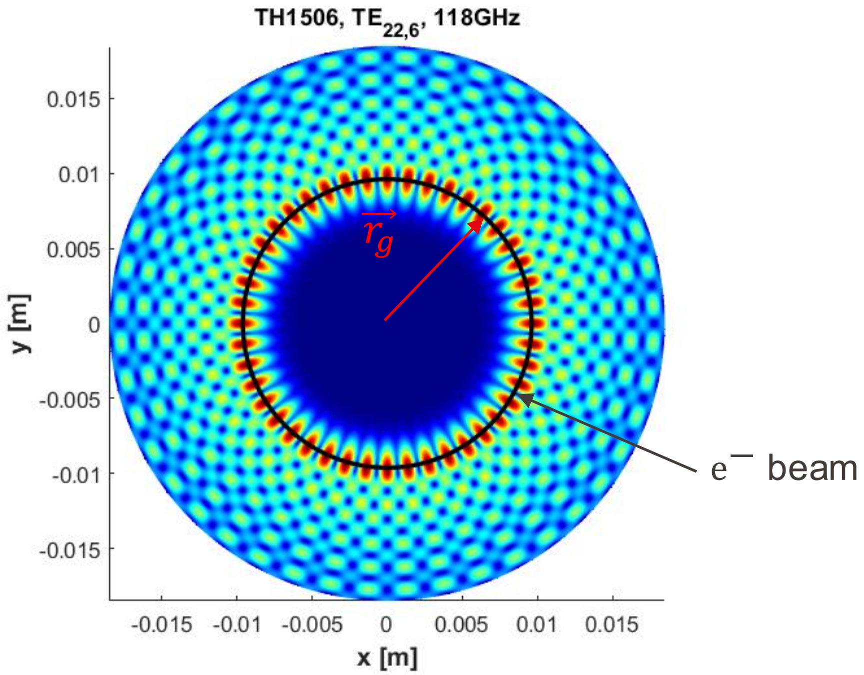

Wave Particle Interaction

- Ideal dispersion relation (**infinite long** cylinder with constant radius)
- The resonance interaction occurs when

$$c\sqrt{k_\perp^2 + k_\parallel^2} = s\frac{\Omega_c}{\gamma} + k_\parallel v_\parallel$$

- Gyrotron: $k_\parallel \simeq 0$

$$\omega_{\mathrm{EM}} \simeq s\frac{\Omega_c}{\gamma}$$

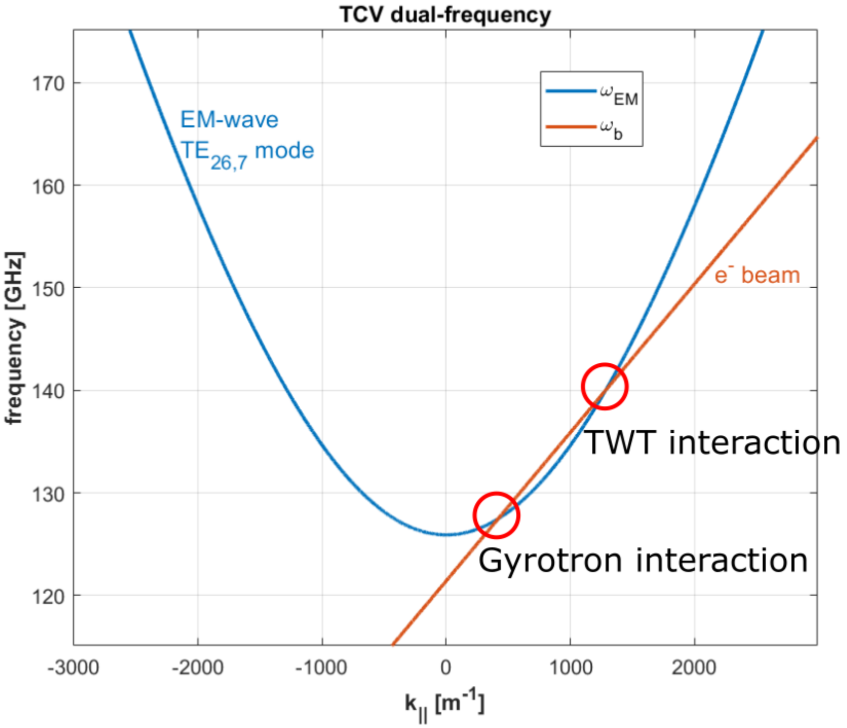

Wave Particle Interaction

- Equation of motion for an electron in an EM field
  - $\frac{\mathrm{d}\vec{p}}{\mathrm{d}t} = -e\left(\vec{E}_{\perp}(\vec{r},t) + \vec{v} \wedge \vec{B}_0\right)$

$\vec{B}_{\perp}(\vec{r},t) \simeq 0$, since $k_{\parallel} \simeq 0$

- Energy exchange for the electron:
  - $\frac{\mathrm{d}W_p}{\mathrm{d}t} = -e\vec{E}_{\perp}(\vec{r},t) \cdot \vec{v}_{\perp}$

Only the perpendicular energy is converted in EM wave energy

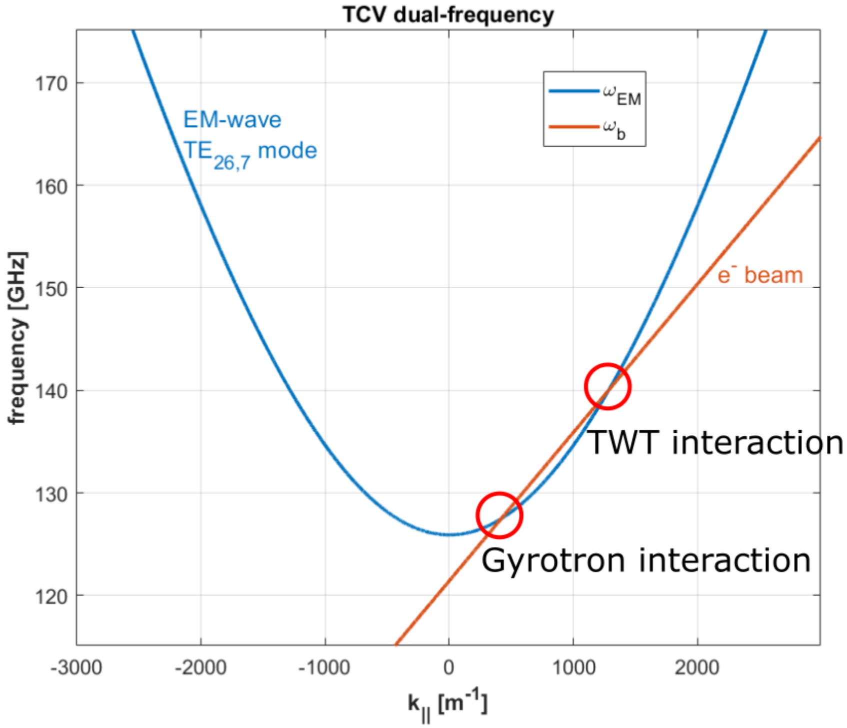

Bunching mechanism

- Depending on the relative phase between the electron gyromotion and the electromagnetic field, electrons may gain or loose energy.
- The relativistic cyclotron frequency depends on energy

$$\Omega_c = \frac{\Omega_{c0}}{\gamma} = \frac{eB_{z0}}{\gamma m_0} \Leftrightarrow \begin{cases} if\ \gamma \uparrow & \Rightarrow & \Omega_c \downarrow \\ if\ \gamma \downarrow & \Rightarrow & \Omega_c \uparrow \end{cases}$$

Negative mass instability

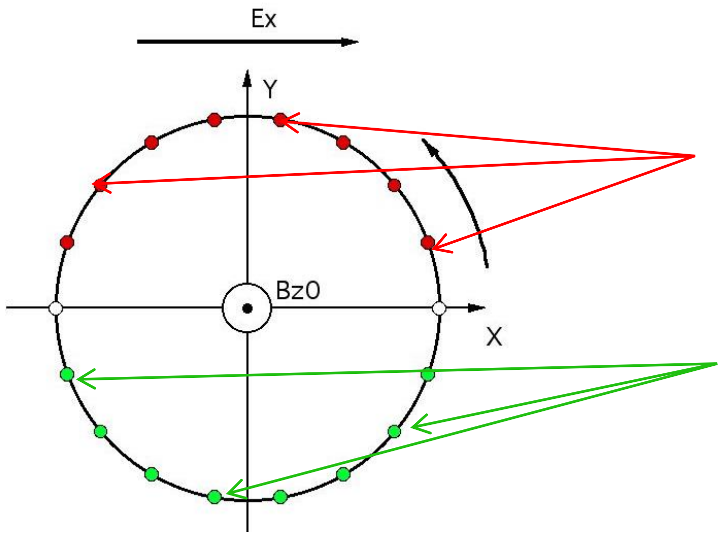

These electrons **gain** energy and will then rotate **slower**

These electrons **loose** energy and will then rotate **faster**

Bunching: Accumulation of particules in a region of phase space

The electron gun

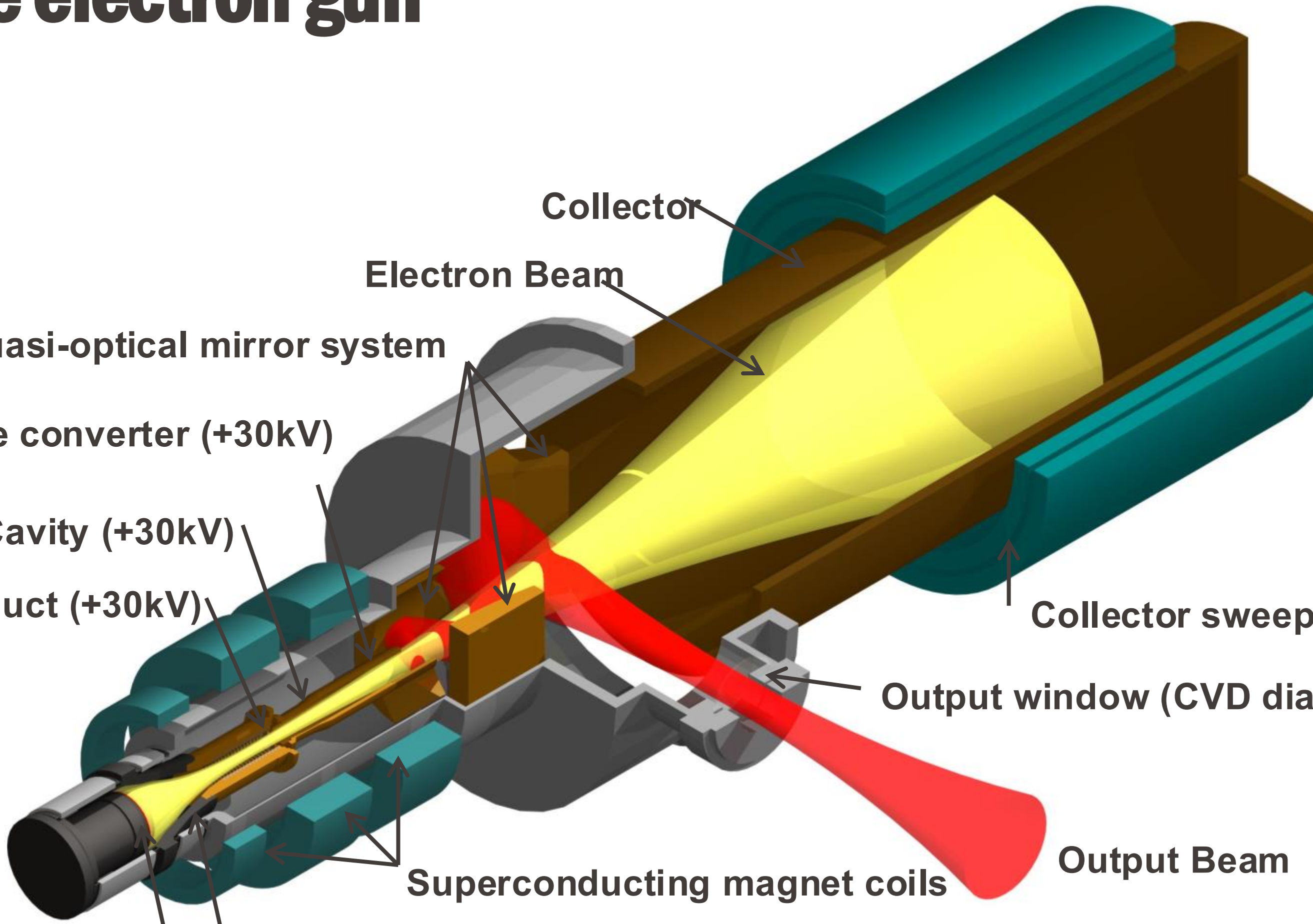

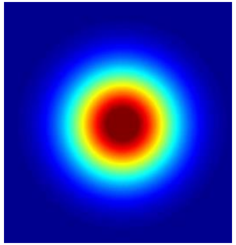

The Magnetron Injection Gun (MIG)

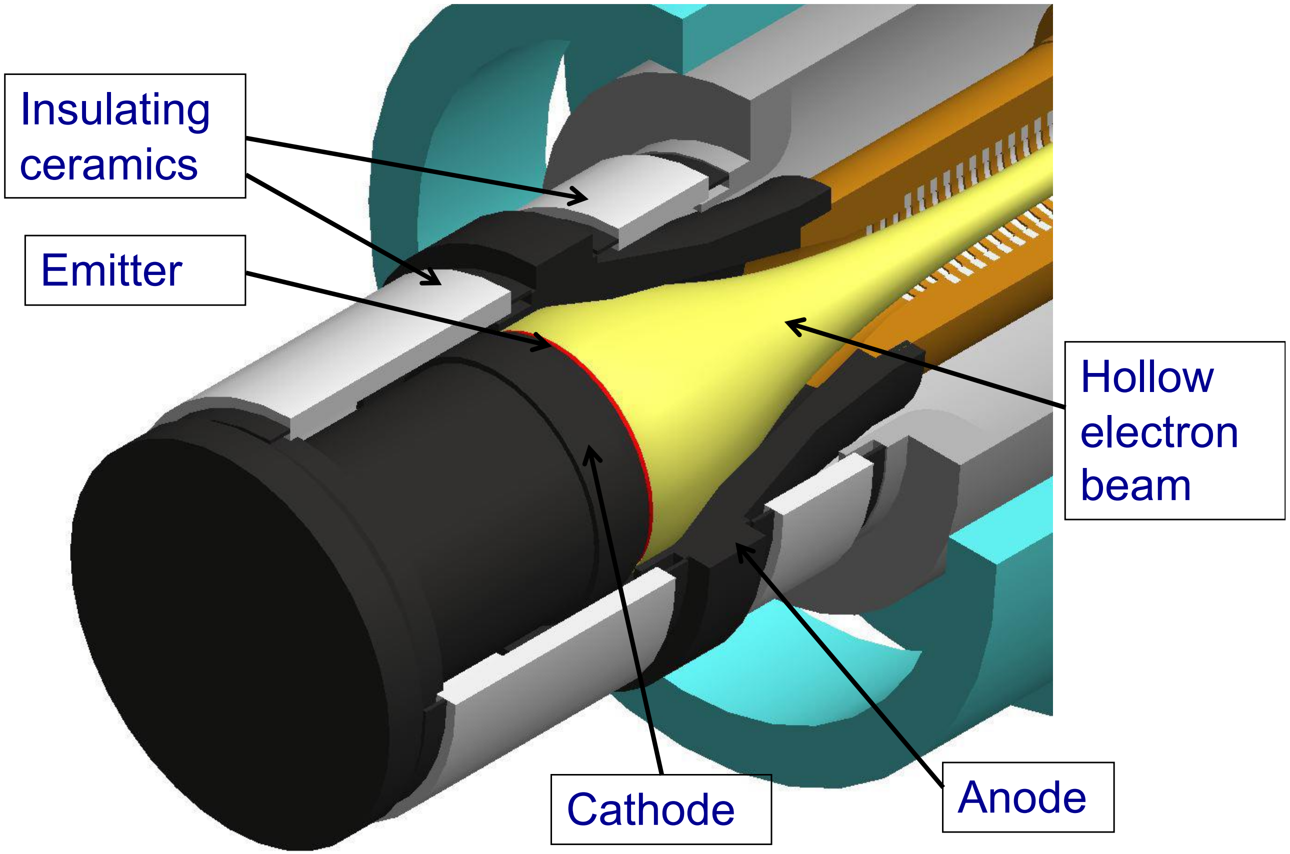

The Magnetron Injection Gun (MIG)

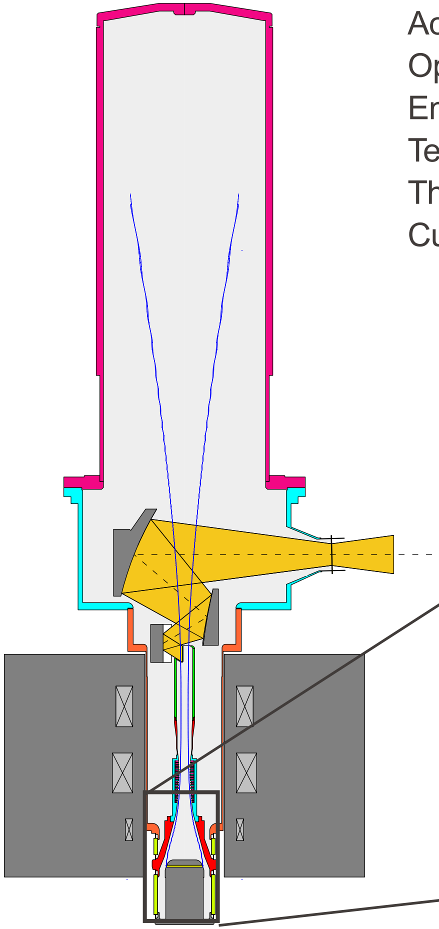

Acceleration Voltage :	80 to 90kV
Operating Current :	25 to 45 Amps (for 1MW RF)
Emitter:	Porous W, with BaO, CaO, Al_2O_3
Temperature:	900-950 °C
Thermalization time:	30-40min
Current density:	< 5A/cm^2

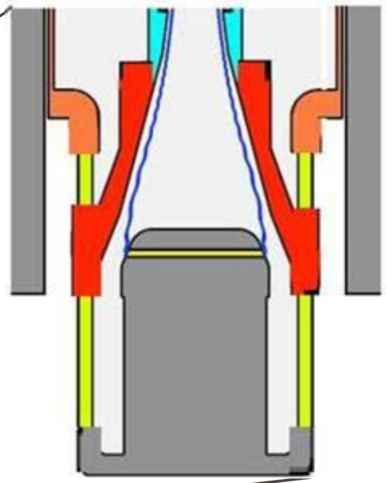

The cathode

- One of the most essential components of all vacuum electron devices, to which the gyrotron belongs. The gyrotron typical warranty (~4000h of filament heating) is essentially determined by the cathode/filament life time.

Table 1.1 Performance data of different types of thermionic cathodes applied in commercial tubes in the sequence of introduction. Lifetime is specified for the DC current densities given

Cathode type	Abbreviation	T_{op} [K]	J_{dc} [A/cm^2]	$e\Phi$ [eV]	Lifetime	References
Tungsten	W	2520	1–4	4.5	>1000 h	Chapter 5
Thoriated tungsten	Th-W	2000	2–4	2.6	10 kh	[1, 80]
Ba oxide	Ox	1050	1–4	1.4	20 kh	Chapter 4, [1, 80]
Ba dispenser, W base	W-I or S or B	1300	3	2.05	≥20 kh	Chapter 2, [1, 80]
Ba dispenser, Os/Ru coating	M or Os/Ru-I	1300	10	1.85	20–130 kh	Chapter 2, [1, 80, 86]
Impregnated Ba scandate	Imp. Scand.	1300	15	1.7	≥10 kh	Chapter 3, [1]
Ba scandate: Sc_2O_3 doped disp.	SDD	1320	40	1.45	≥4000	Chapter 3, [87]

G.Gaertner et al, Modern Developments of Vacuum Electronics, Springer, 2020

The dispenser cathode

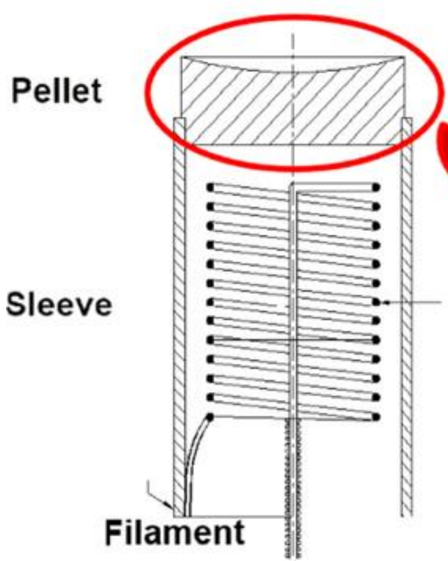

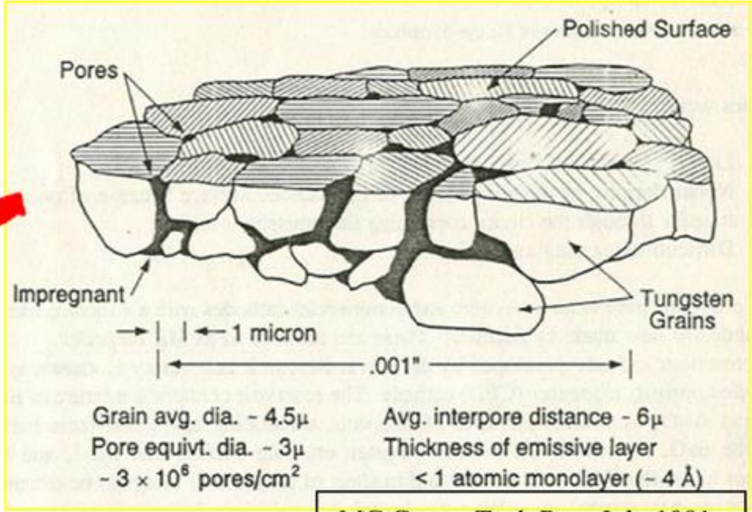

MC Green, Tech Rep, July 1981

A.S. Gilmour, Principles of Traveling wave Tubes, Artech House, 1994

Gyrotron Beam Ducts

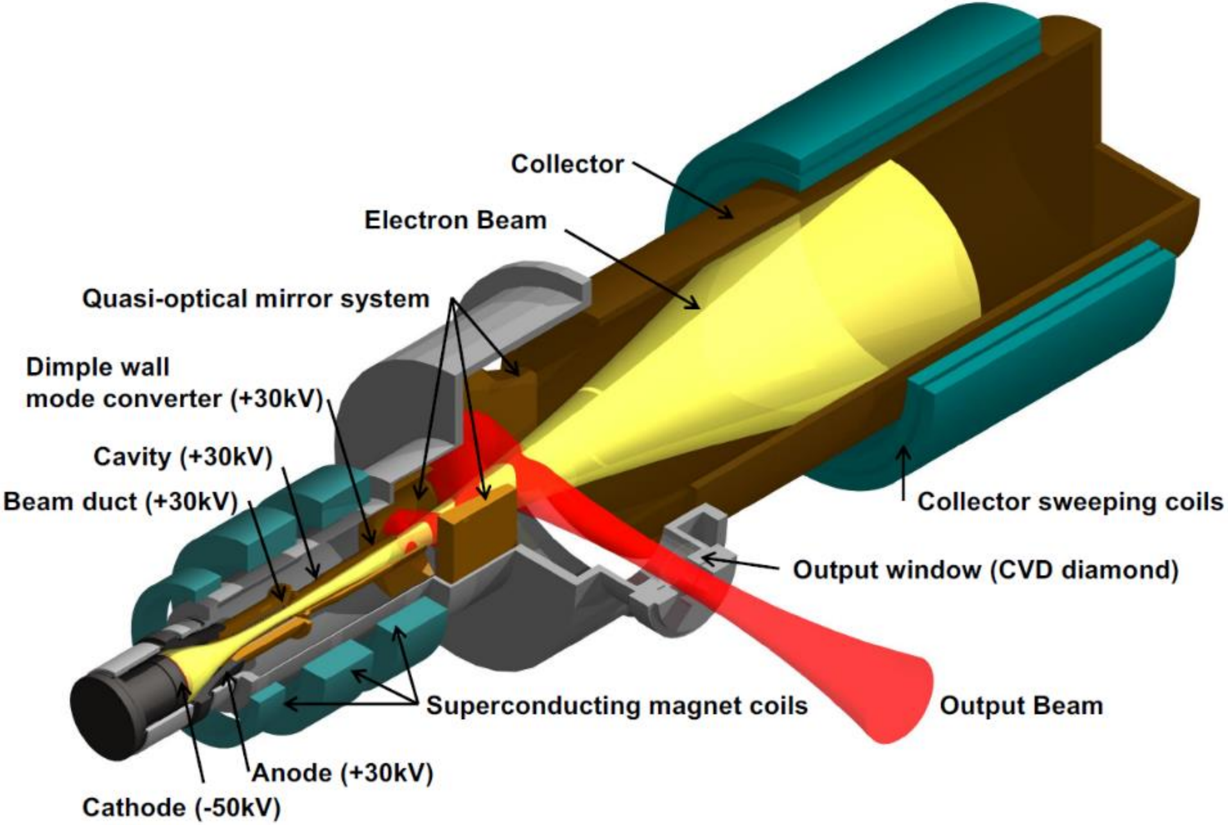

Beam duct strategies

European / USA gyrotrons beam ducts

- Stacked copper and absorbing rings
- Complex asymmetric 3D geometry
- Complex modelisation
- Challenging and costly to manufacture

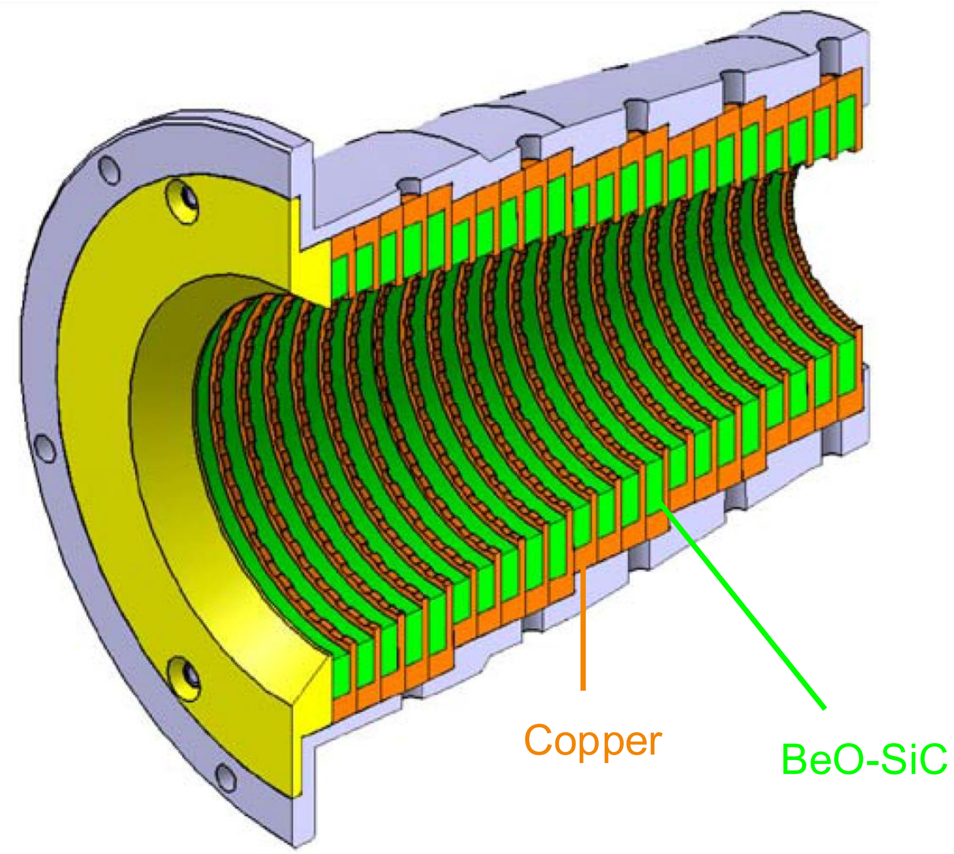

G. Gantenbein, IEEE Trans. on Plasma Science, **38**, 1168 (2010)

EPFL

Beam duct strategies

Japanese gyrotrons beam ducts

- Conical smooth-wall dielectric loaded beam duct
- Successfully used in JAEA high-power gyrotrons
- Cylindrical symmetry
- Much simpler modelisation

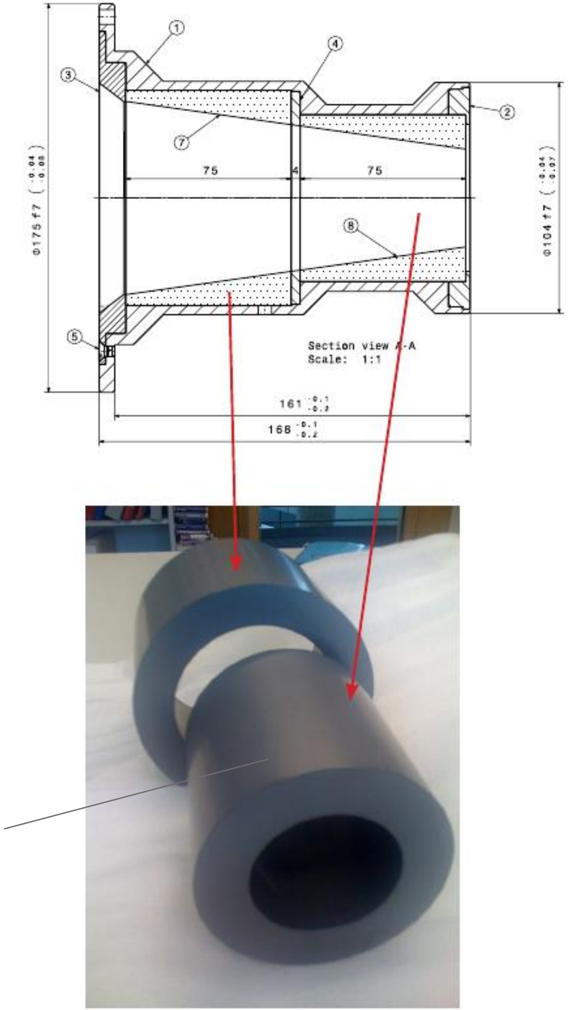

SiC

Swiss Plasma Center

Gyrotron Collectors

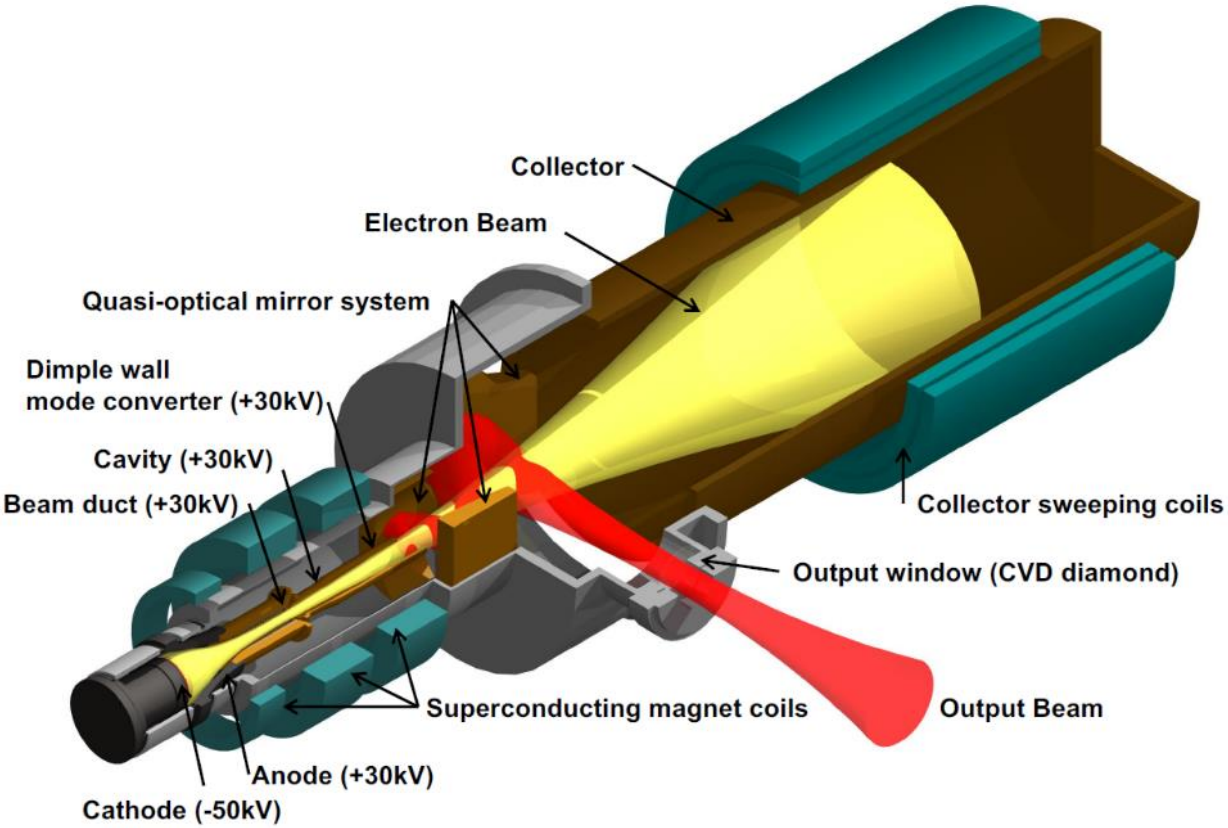

Cooling techniques

Example: Dual-frequency TCV gyrotron (1MW)

- Total dissipated power: 2MW
- Power density: 0.5kW/cm^2
- Thermal equilibration time: 5-6s
- Material: Cu (OFHC)
- Turbulent flow
- Hypervapotron like structure
- Flow (H_2O deionized): 1500l/min
- T_{max} ~ 300°C

Technological limit

- Power density limit: 500W/cm^2 (time-averaged)

- Technological solutions:
  - Material (Cu-OFHC, CuCrZr, GlidCop)
  - Cooling
  - Uniformity of power deposition, electron beam sweeping
  - Depressed collectors (Single stage, Multi-stage)

- Lifetime of the collector
  - Thermo-mechanical fatigue due to cyclic thermal loads

Uniformity of power deposition

- Without any external effect, the electrons from the spent beam are following the field lines of the SC magnet

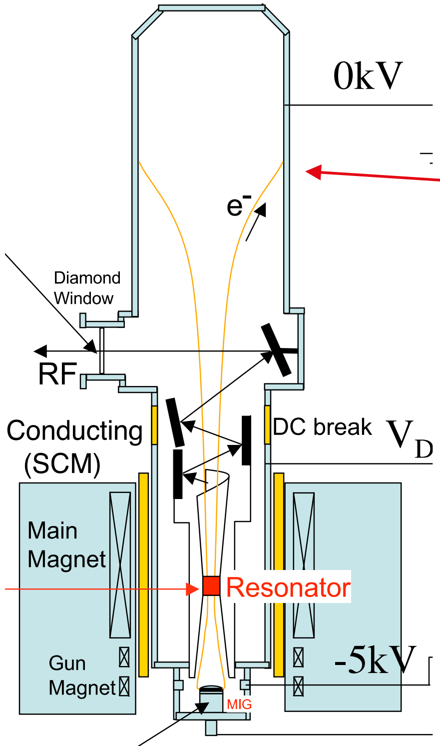

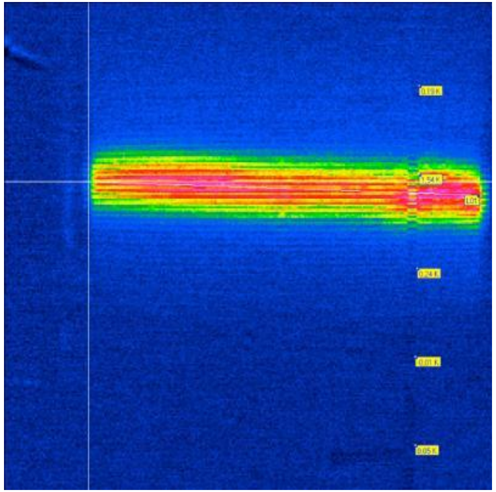

Power density ~ 2kW/cm^2

(Schmid et al. 2007, Dammertz et al. 2005)

Need to spread the power deposition

Different types of collector sweeping systems

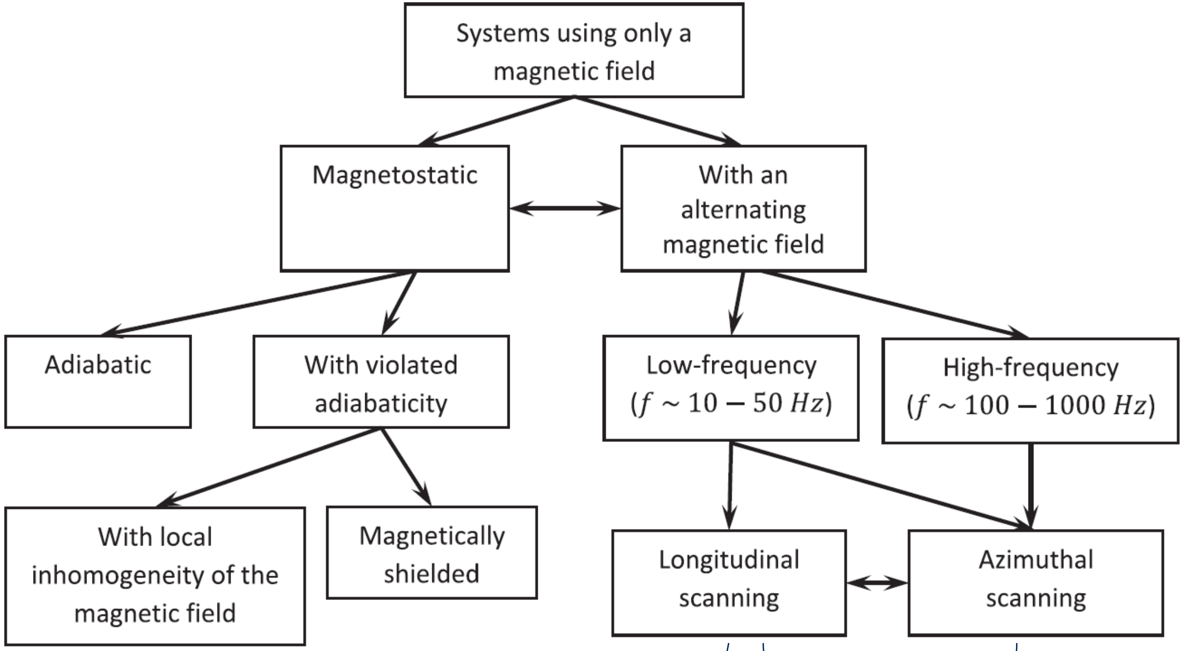

Gycom (TCV 500kW, 82.7 GHz)

TH1506 (TCV 118GHz)
TH1510 (TCV 84/126 GHz)

TH1507 (W7-x)
TH1509U (ITER, DTT)

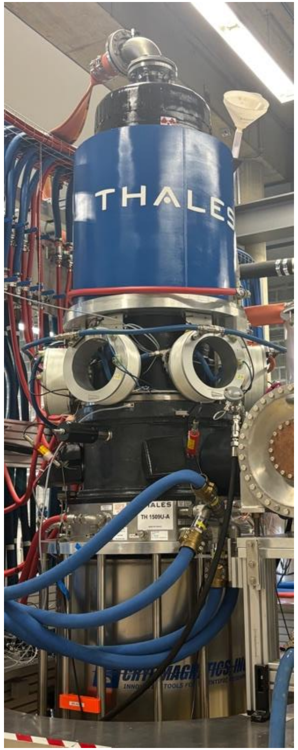

V.N. Manuilov, Gyrotron collector systems: Types and capabilities, Infrared Physics & Technology, 2018

Gyrotron launcher & Internal Optics

- Output coupler
- Separate the spent electron beam from the RF beam
- Convert the $TE_{m,p}$ mode into a Gaussian-Beam $TEM_{0,0}$

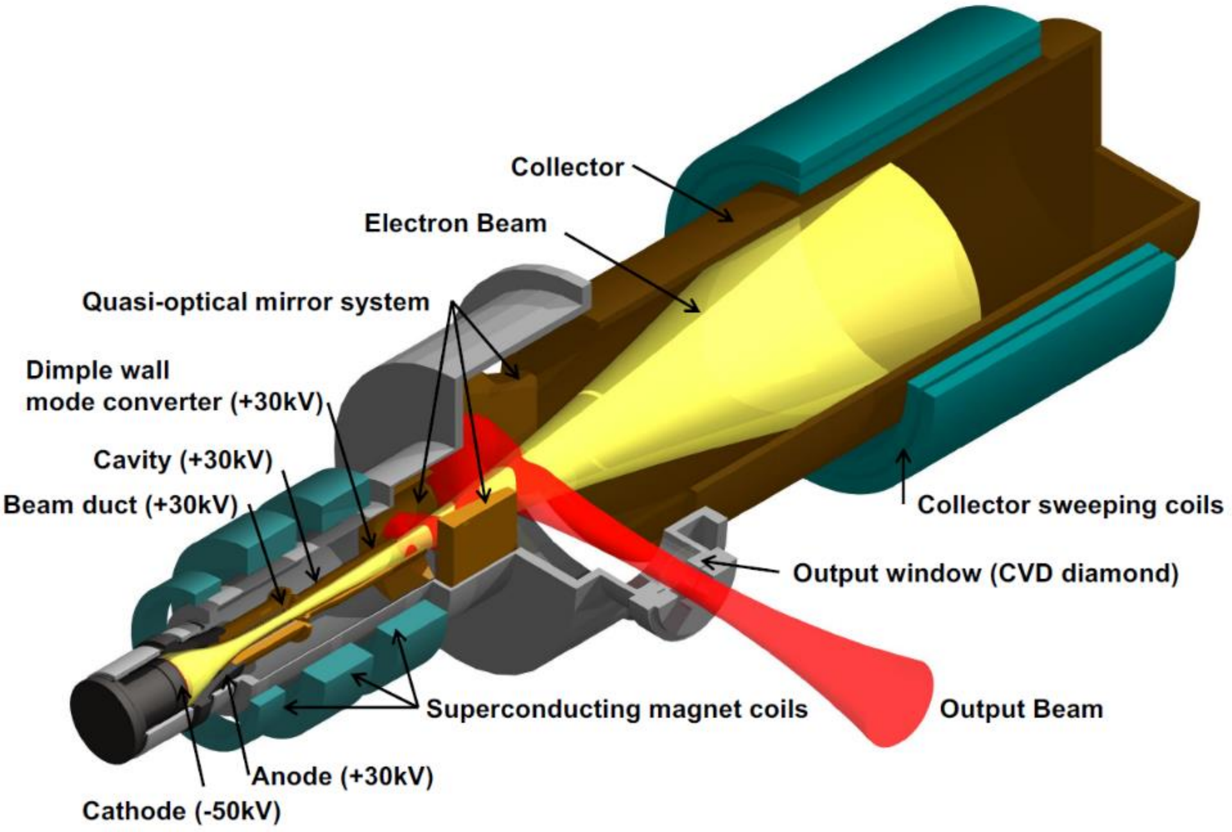

The Mode Converter or Mode Launcher

- Purpose: Convert the $TE_{m,p}$ mode into a nearly Gaussian beam radiating outside the waveguide

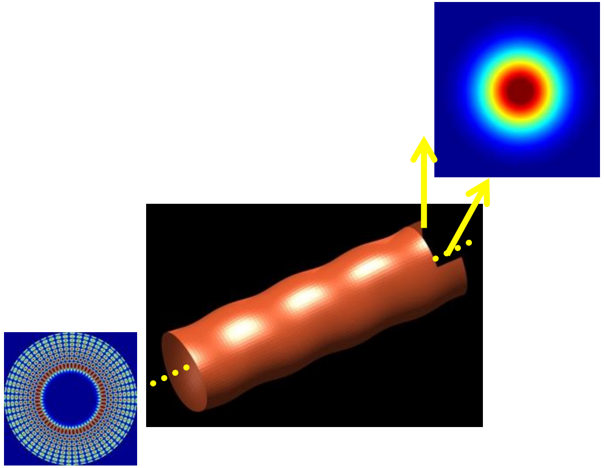

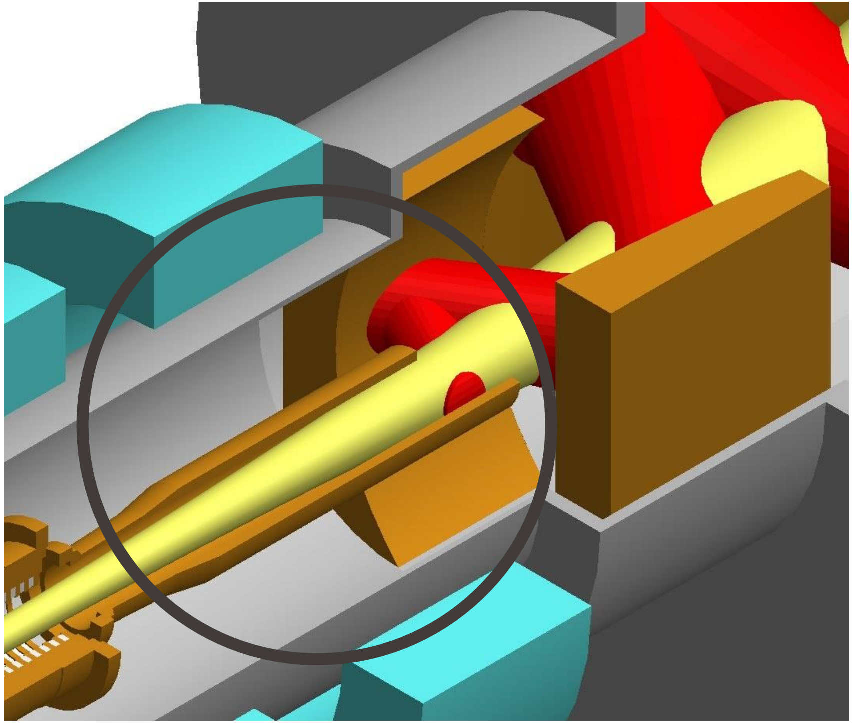

EPFL

The Mode Launcher

- Vlasov launcher
  - Low efficiency of wave conversion (80%)
  - Diffraction effects in the waveguide
  - Need to use quasi-optical theory

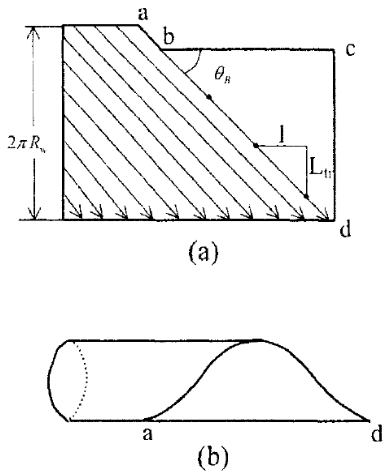

- Dimple-Wall Waveguide Antenna (Denisov launcher)
  - Apply a smooth perturbation to the waveguide surface

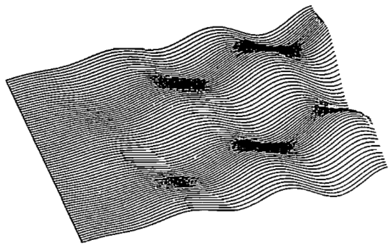

Figure 5. Approximate shape of deformed surface of the waveguide wall.

G.S. Nusinovich, Introduction to the Physics of Gyrotrons, The Johns Hopkins University Press, Baltimore and London, 2004

The Denisov Launcher

- Dimples are used to couple the eigenmode to the smooth waveguide to well chosen adjacent modes
- Concentration of wall current in spots
- Gaussian beam-like radiation pattern

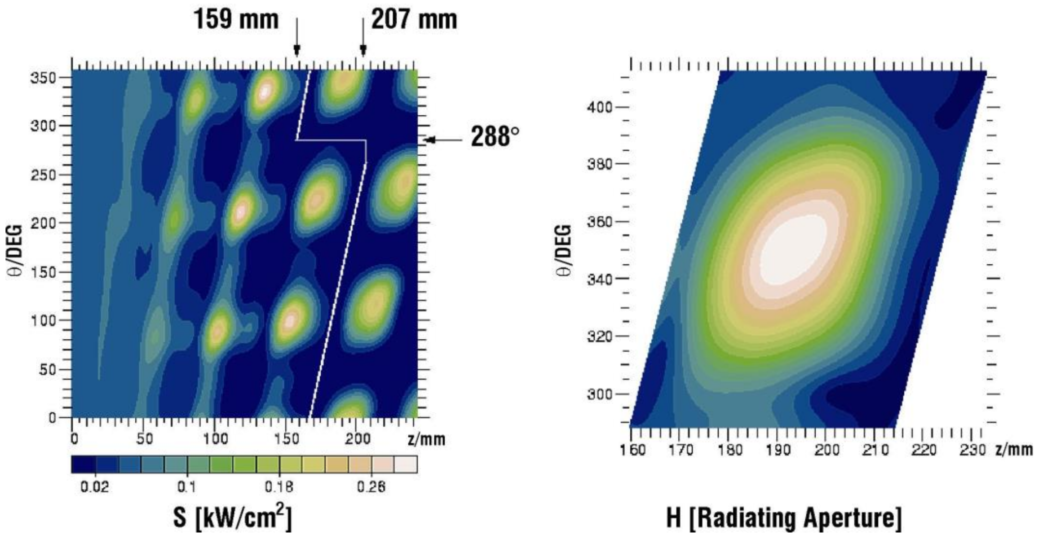

Wall currents in unfolded dimple-wall launcher

Jin et al., "High-Efficiency Quasi-Optical Mode Converter for a 1-MW TE32,9-Mode Gyrotron," in IEEE Transactions on Plasma Science, vol. 41, no. 10, pp. 2748-2753, Oct. 2013

Numerically Optimized Mode Launcher

- Mirror-line launcher
- Consider each Brillouin zone as a 'mirror'. Synthesize each surface to optimize output.

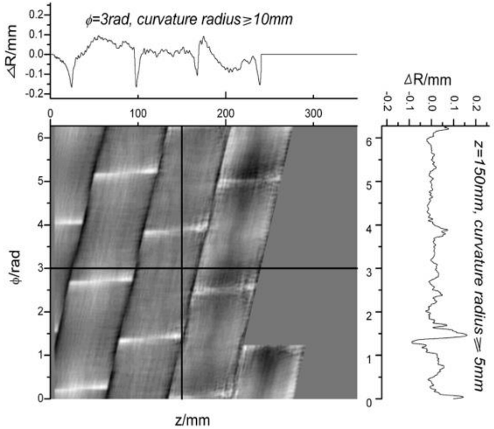

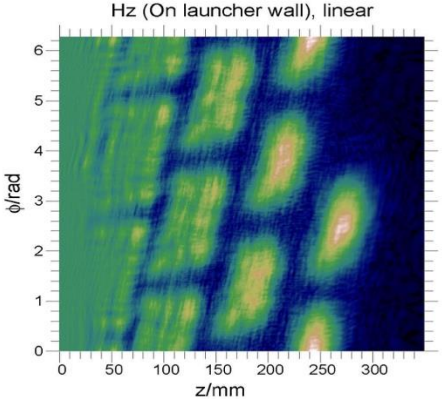

- Fundamental Gaussian mode content: 96.26% at launcher aperture.
- Perturbation Δr: -0.22mm< Δr<0.26mm.

Swiss Plasma Center

J. Jin et al., 16th Joint Workshop on Electron Cyclotron Emission and Electron Cyclotron Resonance Heating (EC16), Sanya, China, April 12-15, 2010

The Quasi-Optical Mirror System

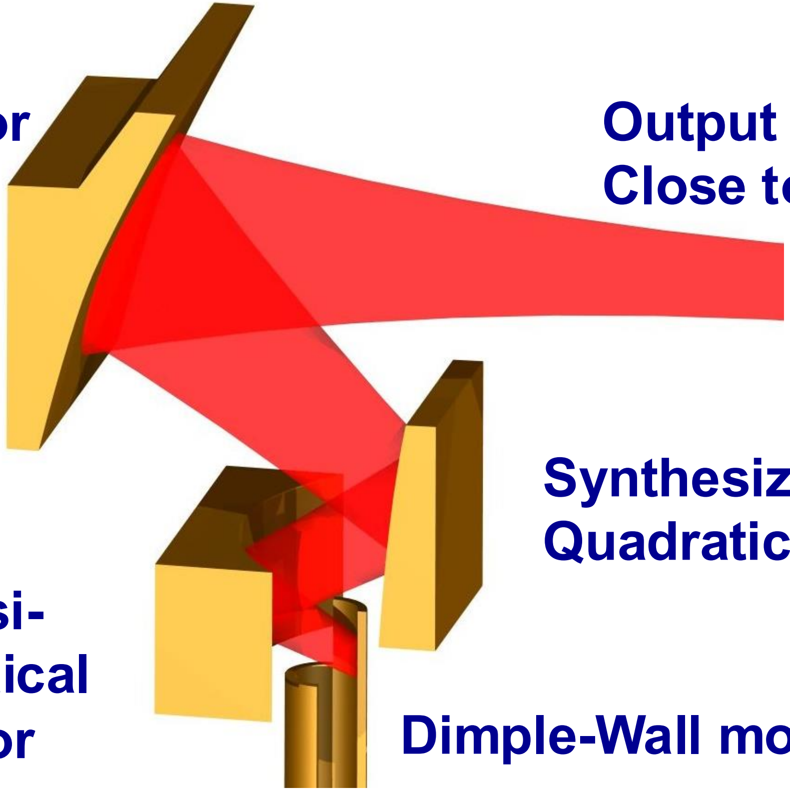

- Purpose: Direct output beam to window, maximizing the Gaussian content and minimizing trapped (stray) radiation

Gyrotron Window

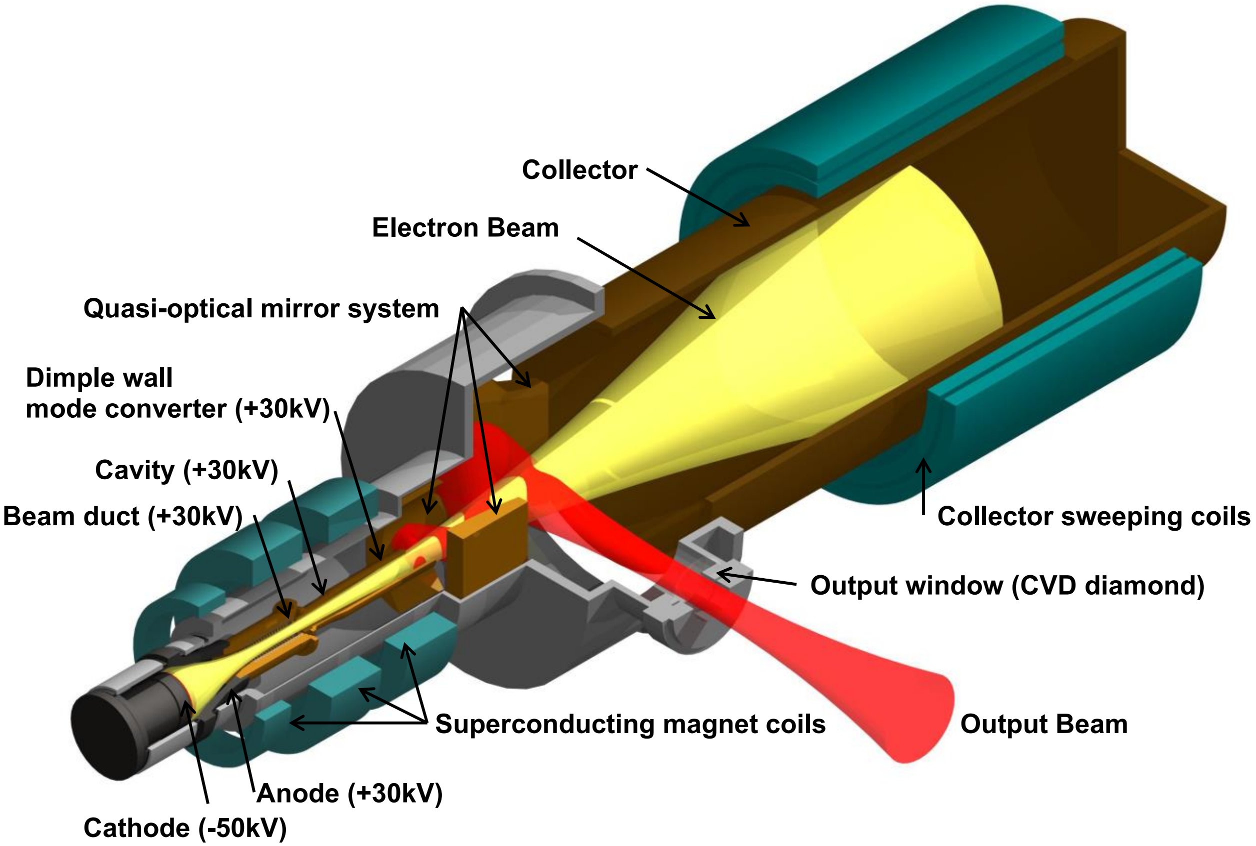

The window

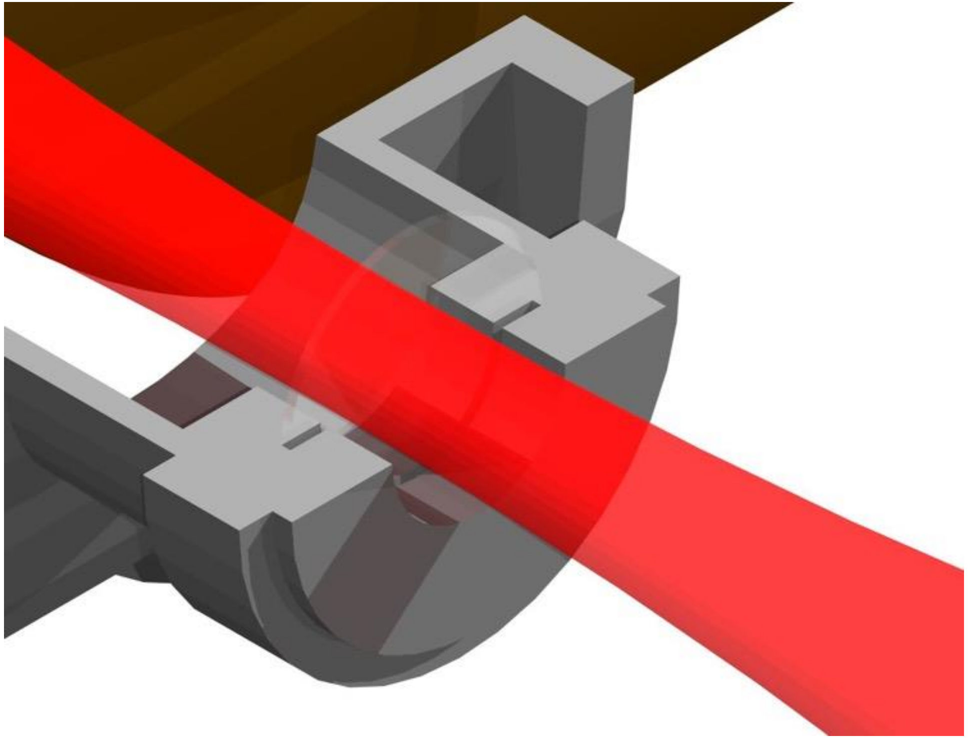

- The window acts as a vacuum barrier between the extremely good gyrotron vacuum <10^{-8}-10^{-9} mbar) and the outside world.
- The power distribution at the window is Gaussian.
- The absorption is extremely low for CVD diamond
- The polarization of the wave is linear (horizontal for a gyrotron mounted vertically)

The window

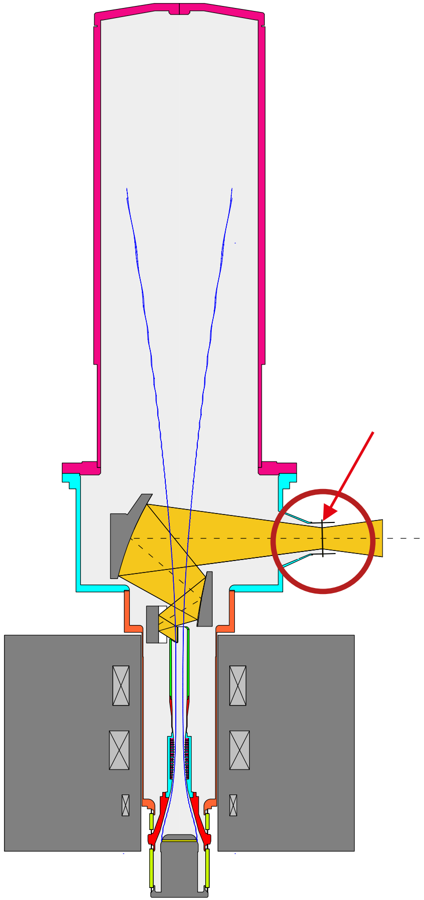

Role: Vacuum barrier

Material: CVD diamond

Losses: Few tens of W (Tan δ: $1.\ 10^{-5}$ - $1.\ 10^{-4}$)

Permittivity: $\varepsilon = 5.7$

Thermal conductivity: $\sigma \sim 2000$ W/m/K

Difficulty: High temperature Brazing,
Cu and diamond thermal expansion coeffs are very different.

Unit price: ca. 100k€

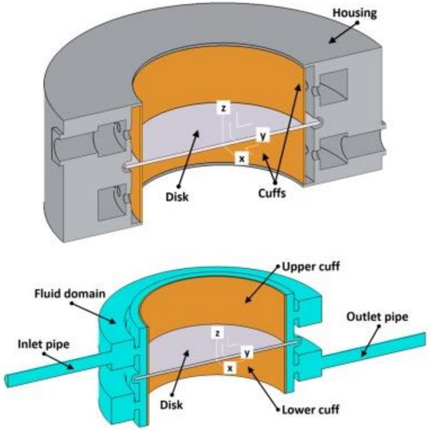

G. Aiello, Fusion Engineering and Design, 2021

Swiss Plasma Center

Window transmission/absorption properties

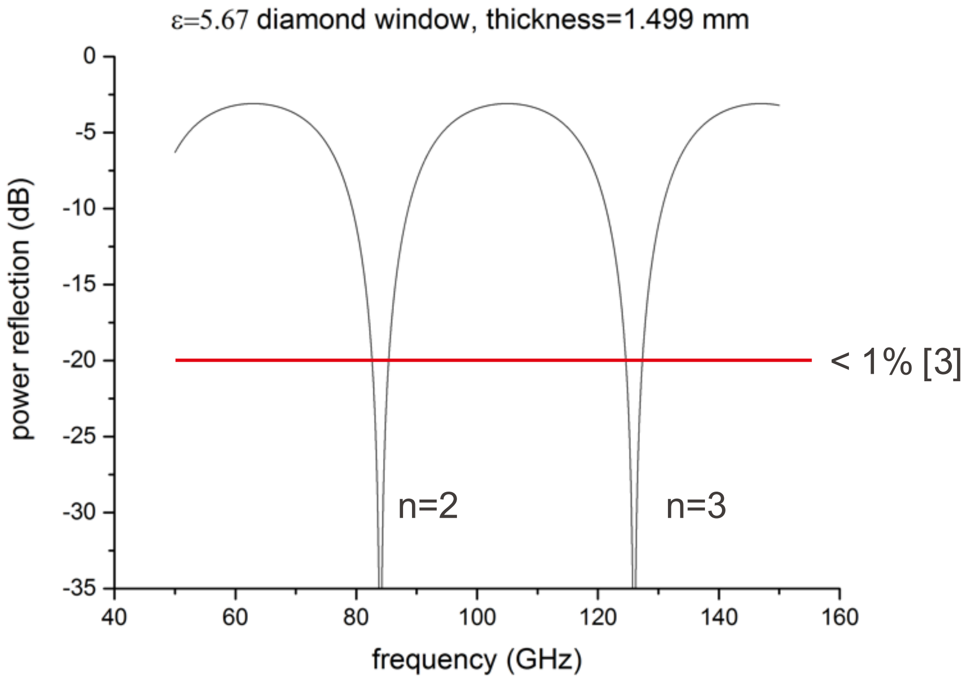

- For a single disk gyrotron-window, the window transmission is optimal at a discrete frequencies defined by:

$$f_n = \frac{c}{\sqrt{\epsilon_r}2d}\ n\ [Hz]$$

d: window thickness

c: speed of light

ϵ_r: dielectric permittivity

n: integer

Gyrotrons for ITER

- ITER requirement:
  - P = 1 MW for 3600s
  - Frequency: 170 GHz
  - Global efficiency: 50%
  - 5kHz full power modulation

Europe

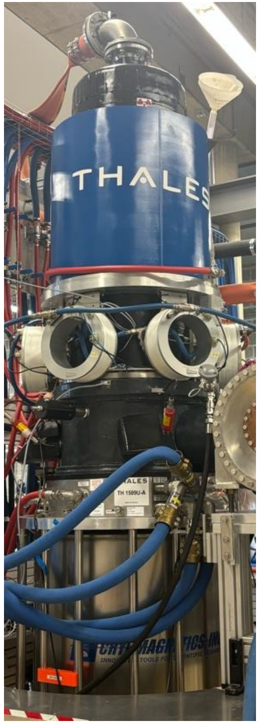

Japan

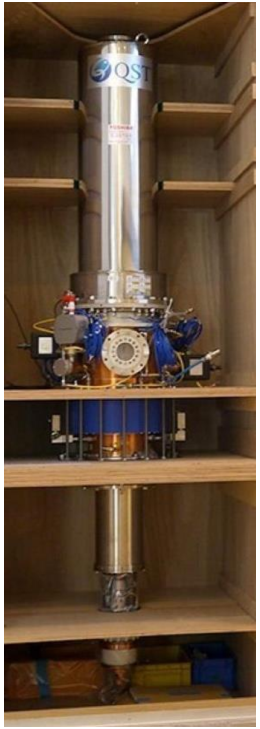

Russia

Development and challenges

- Increase of power or frequency: P > 1.5 MW f > 200 GHz ?
- Improvement of the efficiency: 60-70 % ?
- Multi-frequency gyrotrons
- Improvement of the reliability
- Industrialisation

Power/Frequency increase

- Some power is dissipated in the interaction region (cavity) due to ohmic loading
- The cooling technology limit is 2.5 kW/cm^2
- Challenge: the power dissipated in the cavity scales as $f^{5/2}$
- Increasing the radius would decrease the dissipated power density, but increase the probability of mode competition (overmoded structure)

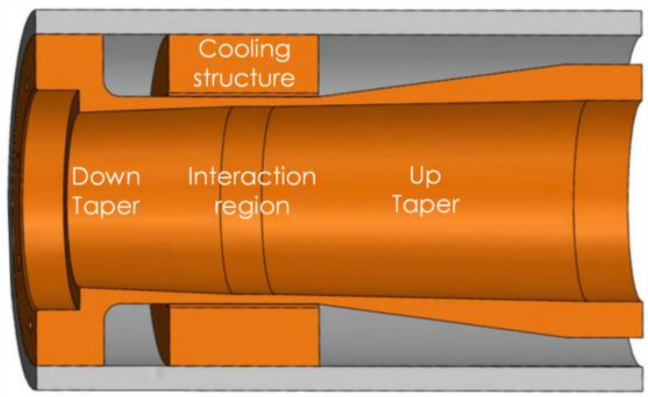

Monomode system: TE_{10} - rectangular

- Example of fundamental WR6.5 waveguide

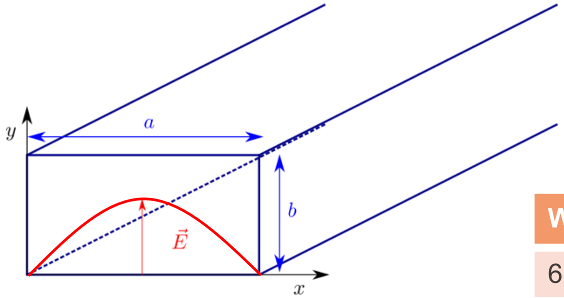

$$\vec{E}(x,t) = E_0\, sin(k_\perp x)\, e^{i(\omega t - k_\parallel z)}\, \vec{e}_y$$

$$k_\perp = \frac{\pi}{a}$$

WR	a	b	frequency
6.5	1.65 mm	0.825 mm	110-170 GHz

- Examples of applications:

Swissto12®

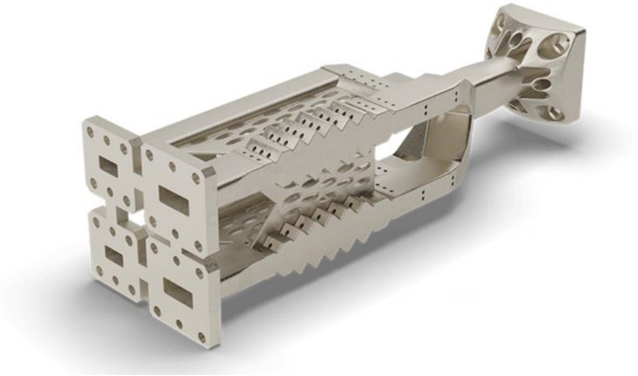

High power gyrotrons are strongly overmoded structures

DNP gyrotron (263GHz, 150W, $TE_{7,2}$)
R = 2.5 mm

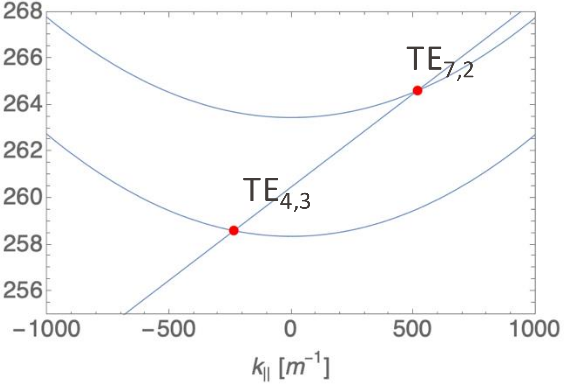

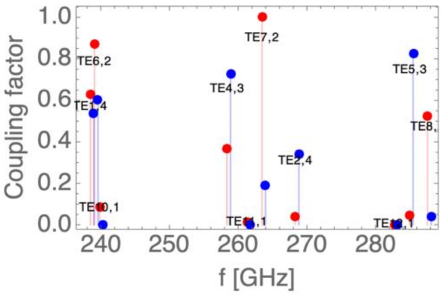

Weakly overmoded

ITER EU gyrotron (170GHz, 1MW, $TE_{32,9}$)
R = 20mm

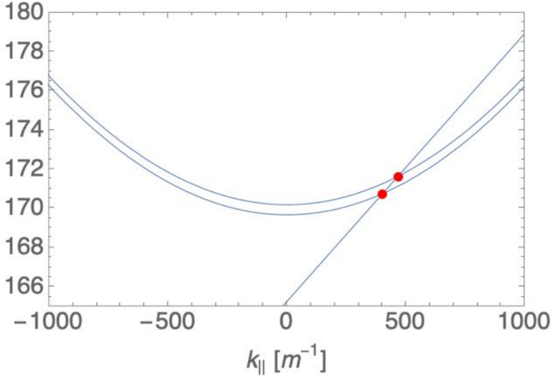

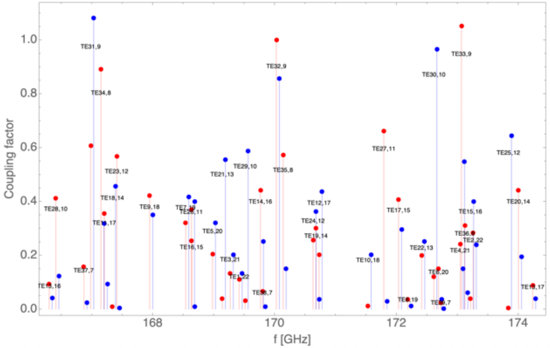

Strongly overmoded

Swiss
Plasma
Center

Improvement of the efficiency, SSDC and MSDC

- Single Stage Depressed Collector (SSDC)
- Main idea: Reduction of the installed electrical power
  - Increase the total efficiency
  - Reduce the collector wall loading
- Example of gyrotron without depression scheme

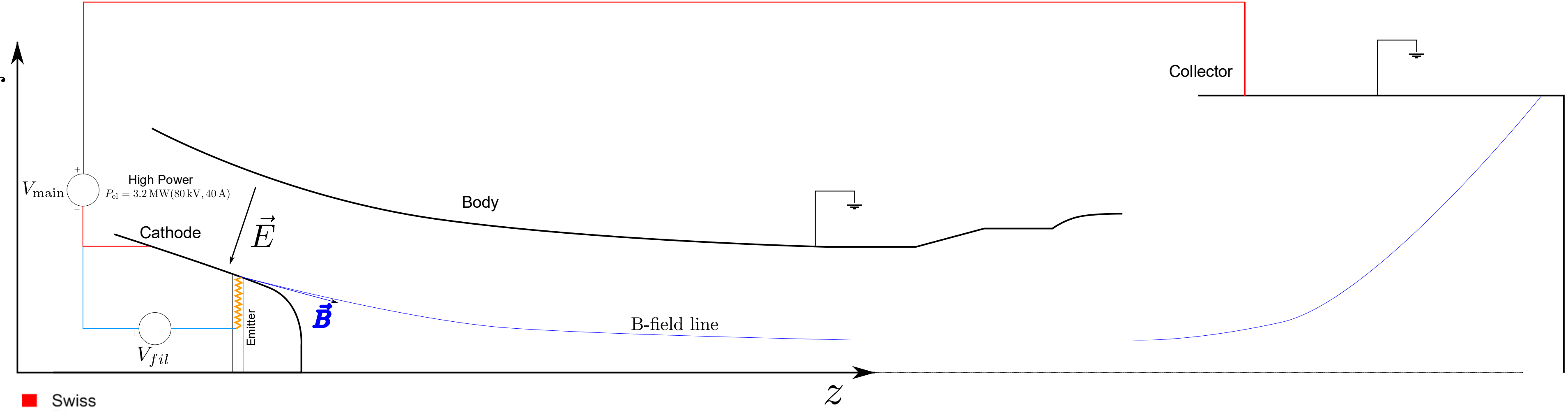

Improvement of the efficiency, SSDC and MSDC

- Single Stage Depressed Collector (SSDC)
- Main idea: Reduction of the installed electrical power
  - Increase the total efficiency
  - Reduce the collector wall loading
- Example of gyrotron with a SSDC depression scheme

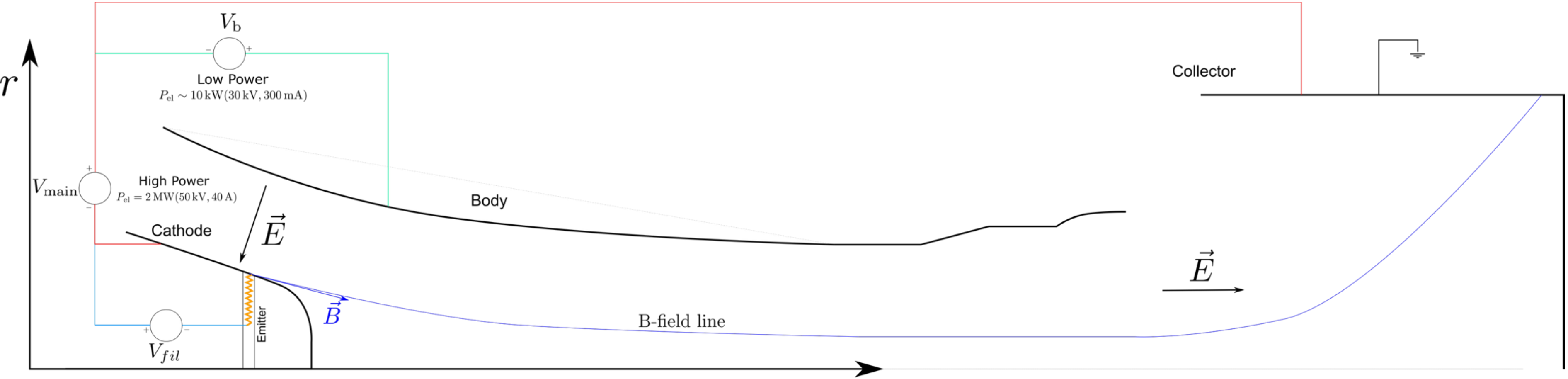

Improvement of the efficiency, SSDC and MSDC

- The depression voltage is limited by the lowest kinetic energy of the electrons
  - Avoid electron reflections towards the gun
  - Set the maximum total efficiency (~50%)

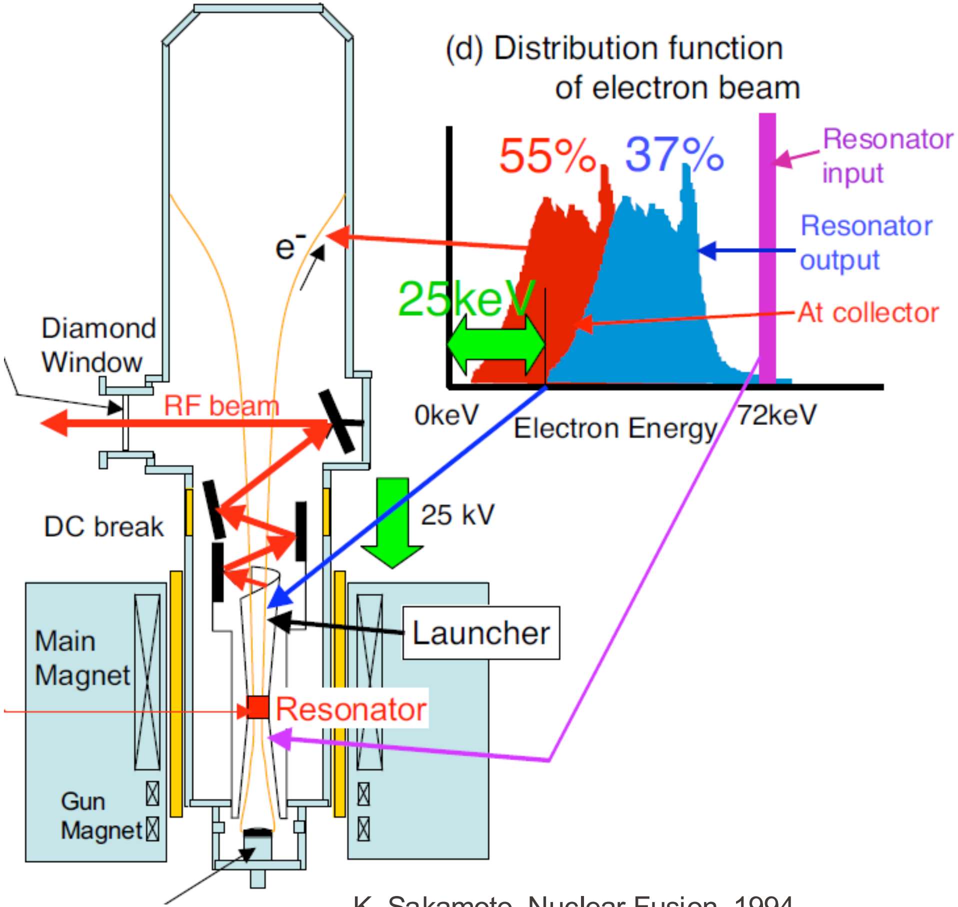

K. Sakamoto, Nuclear Fusion, 1994

Multi-Stage Depressed Collectors (MSDC)

- Advanced concept of beam collection
  - Increase further the efficiency
  - Decrease the heat load
- Different concepts
  - Magnetic field
    - Non adiabatic transition
    - Azimuthal magnetic field
  - Electric field
    - Electrostatic lenses (TWT)
    - Cross-fields

Multi-Stage Depressed Collectors (MSDC)

- Cross-fields depressed collector
  - Most promising concept
  - Sort the electrons according to their kinetic energy

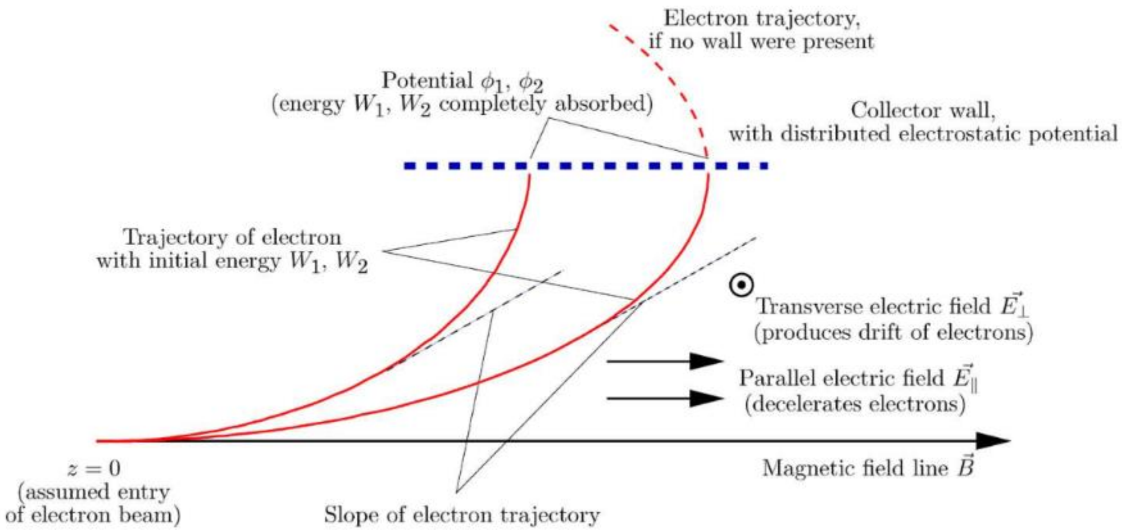

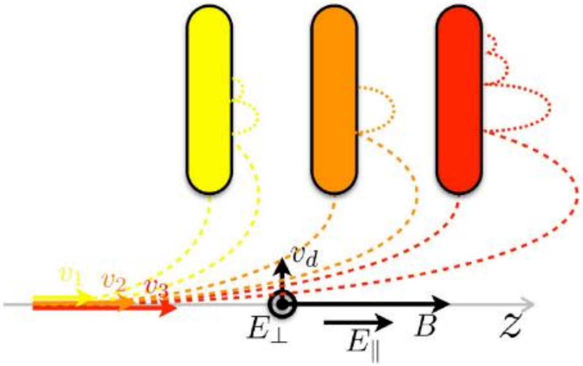

I. G. Pagonakis et al., IEEE Transactions n Plasma Science, Vol. 36, No. 2, April 2008

Multi-Stage Depressed Collectors (MSDC)

B. Ell et al., Realization of the First MW-Class Gyrotron Multistage Depressed Collector, PhD thesis, KIT, 22.07.2025

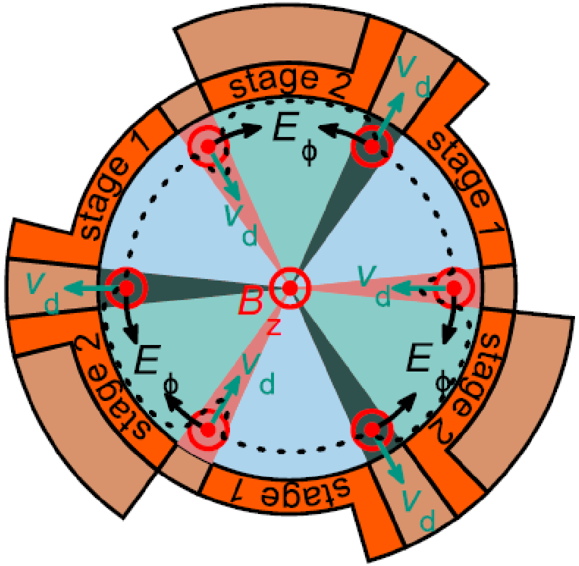

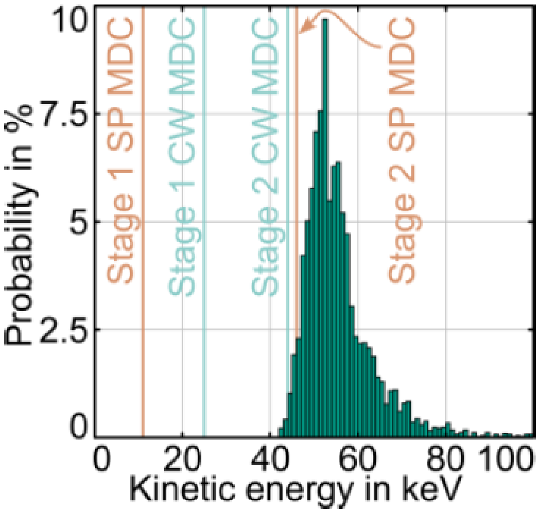

- Very promising concept
  - Calculated efficiency up to 65%
- Challenging manufacturing

B. Ell et al., IEEE Transactions on Electron Devices, vol. 70, no. 3, March 2023

Gyrotron Efficiecy with Depressed collector

Internal RF losses (ohmic + diffractive)

Electronic efficiency (gyrotron physics) weak margin of improvement

$$\eta_{gyro} = \frac{\epsilon_{out}\,\eta_{el}}{1 - \eta_{col}(1 - \eta_{el})}$$

Total gyrotron efficiency

Depressed Collector efficiency
possible margin of improvement

$\eta_{el} = 35\%$

$\varepsilon_{out} = 90\%$

$\eta_{col,ss} = 50\%$ (single-stage)

$\eta_{col,ms} = 65\%$ (multi-stage)[1]
(theoretical value, to be demonstrated experimentally)

- Gyrotron efficiency can be increased by developping the multi-stage depressed collector

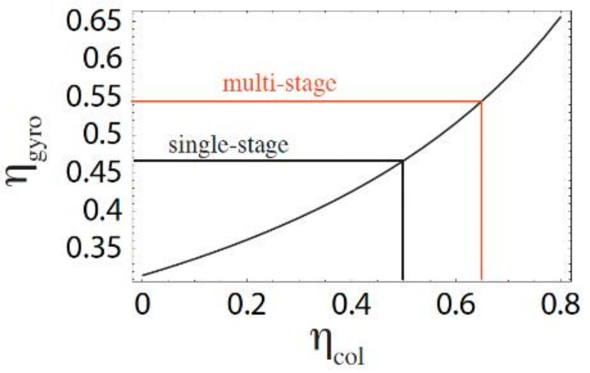

[1] G. Ling et al., IEEE Trans. Plasma Science, Vol.28 (2000), p.606

Multi-Frequency gyrotrons

- Quasi-Optical mode converters can be designed for more than one mode
- Example: QST ITER gyrotron
- The cavity is capable of exciting many different $TE_{m,p}$ modes by varying the beam parameters
  - R_b
  - Pitch factor
  - Cyclotronic frequency
- The QOMC is much more selective

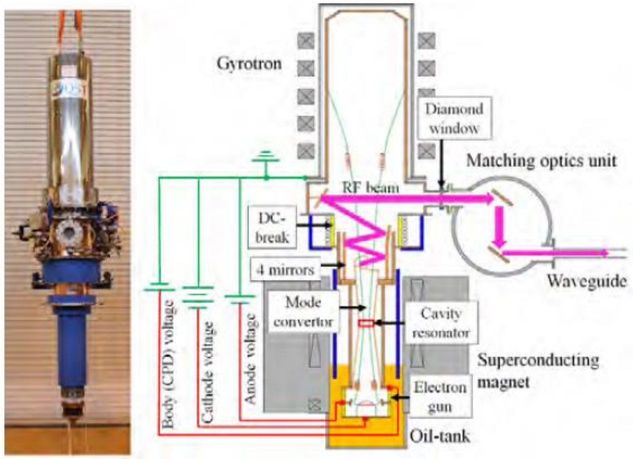

Figure 1. Appearance of gyrotron tube and a schematic view of gyrotron complex with a matching optics unit.

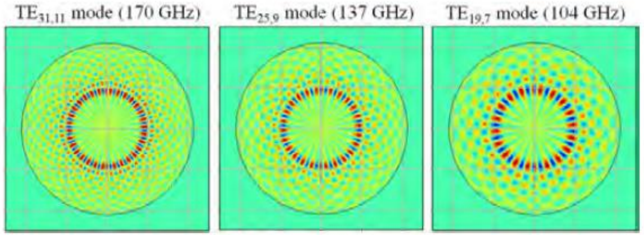

Figure 2. Electric field distributions of $TE_{31,11}$, $TE_{25,9}$, and $TE_{19,7}$ modes in cavity resonator (radius 20.87 mm).

R. Ikeda, Nuclear Fusion, 2023

Swiss Plasma Center

Multi-Frequency gyrotrons

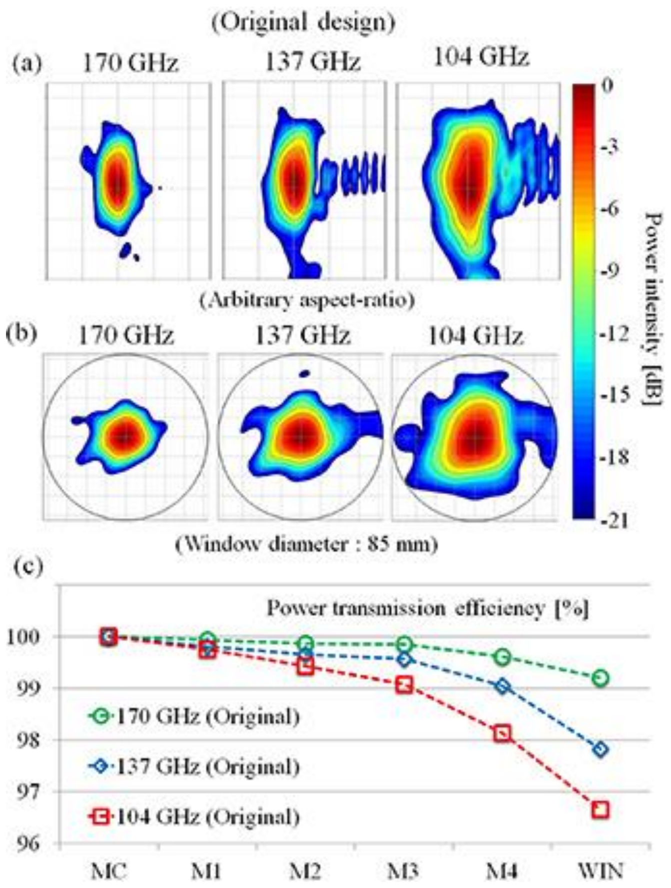

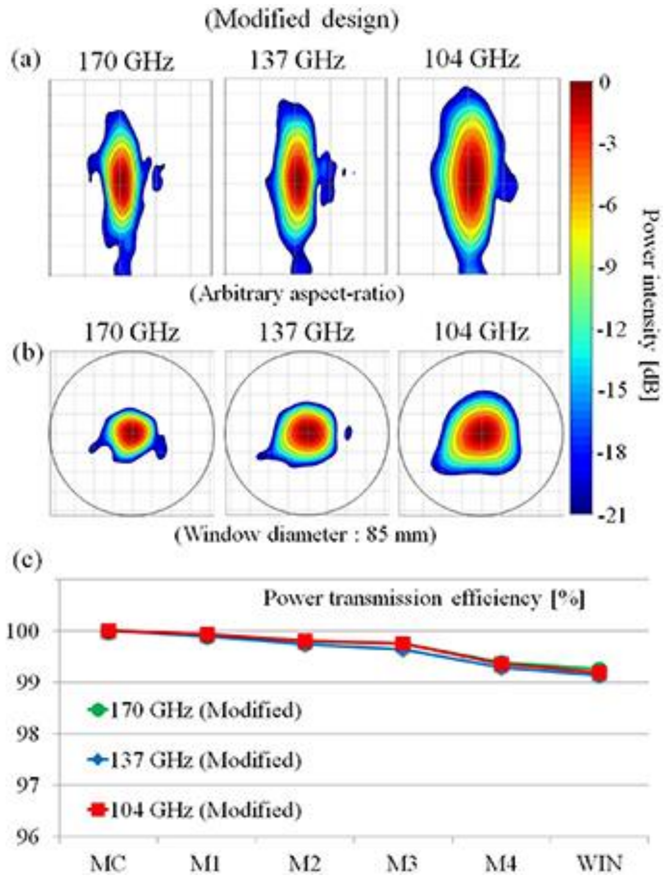

R. Ikeda, Nuclear Fusion, 2023

ITER external heating systems

<u>Outline</u>

- 1. Sources
- 2. Transmission lines and components
- 3. Launchers

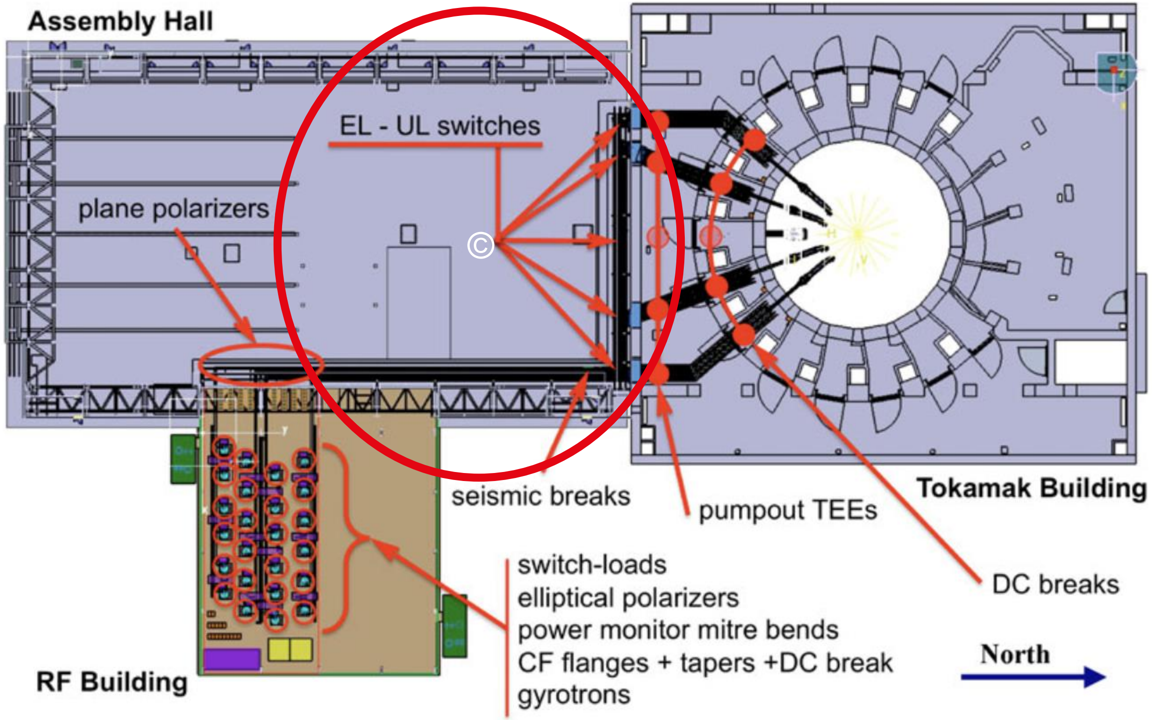

F. Gandini, Fusion Science and Technology (2010)

Types of propagation

- Waveguide, Transmission lines (ITER, DIII-D, HL-3, TCV)
  - Linearly polarized modes $LP_{01} \equiv HE_{11}$
  - Ref: E. J. Kowalski et al., Linearly Polarized Modes of a Corrugated Metallic Waveguide, IEEE-TMTT, 58 (2010)
- Free space, quasi-optical propagation (W7-X, DTT, DEMO)
  - Linearly polarized modes $TEM_{00} \equiv$ Gaussian mode
  - Ref: G. Michel, Matching of the ECRH transmission line of W7-X, Fusion Engineering and Design (2012),

Quasi-Optical propagation, W-7X

- 10 Gyrotrons
- 40m Quasi-Optical transmission line (atm pressure)
- 10 single-beam WG
- 2 multi-beam WG
- Diamond windows at the two interfaces (gyrotron and plasma)

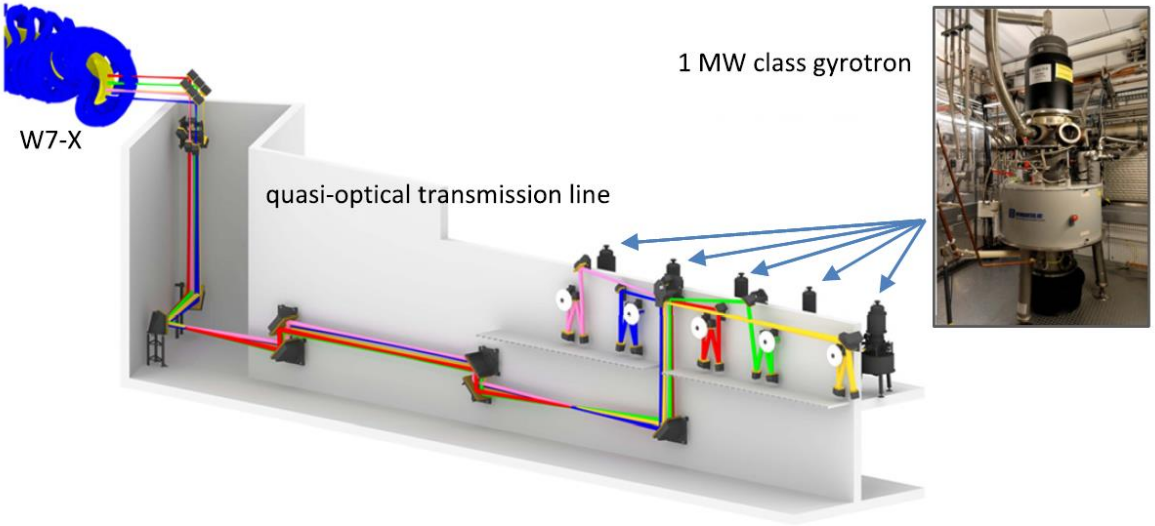

H.P. Laqua, 2021 [8]

95% efficiency

Waveguide, Transmission line, ITER

- Tritium handling (nuclear plant) → HE_{11} waveguide
- Requirement: ≥ 90% transmission efficiency
- Multiple TL components:
  - DC breaks
  - TEM_{00} to HE_{11} coupler
  - Miter Bends (MB) and Polarizers
  - Switches
  - Loads
  - Pump-out sections
  - Valves

Gandini et al. EC H&CD TRANSMISSION LINE FOR ITER

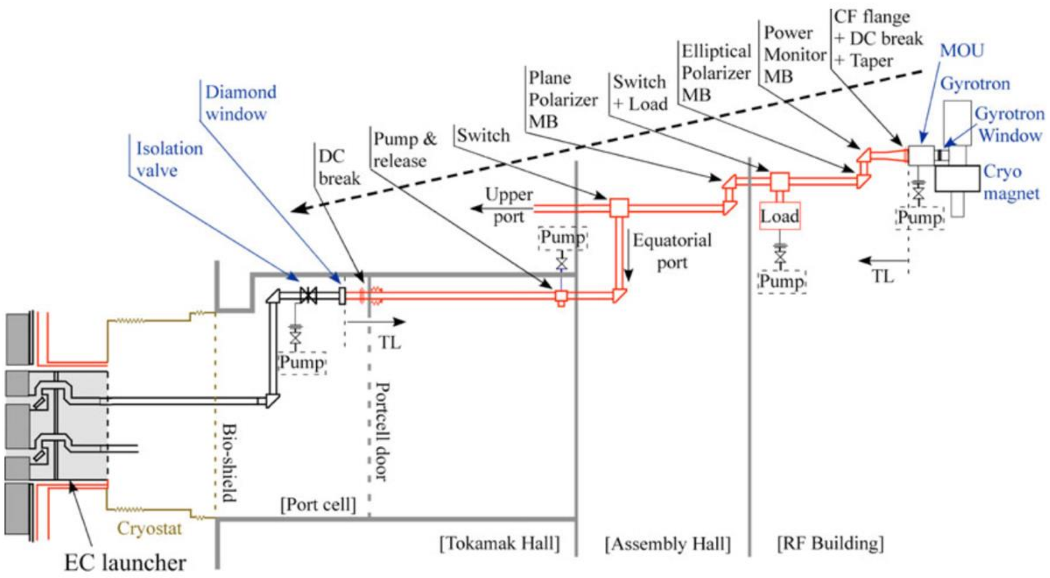

Fig. 1. Schematic of a generic TL.

F. Gandini, 2010 [10]

Matching Optics Unit (MOU)

- Couple the wave to the transmission line
- Shape the beam exiting the gyrotron to optimize the coupling to the HE11 mode in the transmission line
- Minimize higher order modes

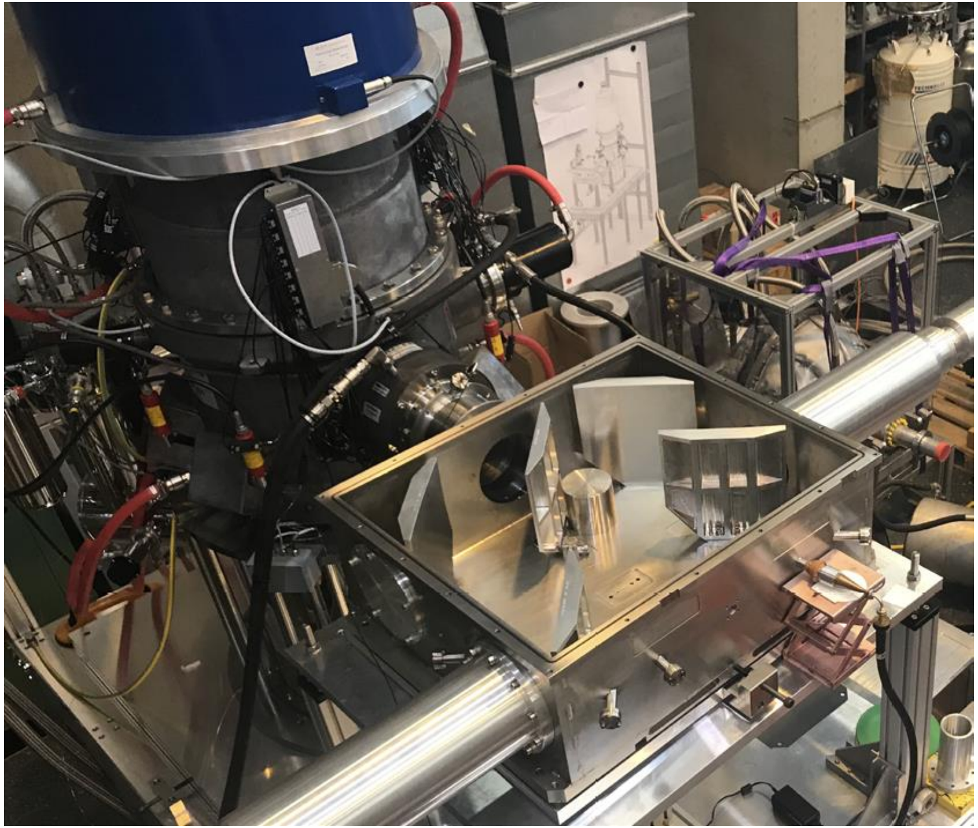

Waveguide, Transmission line, ITER

- Transmission lines (Aluminium)

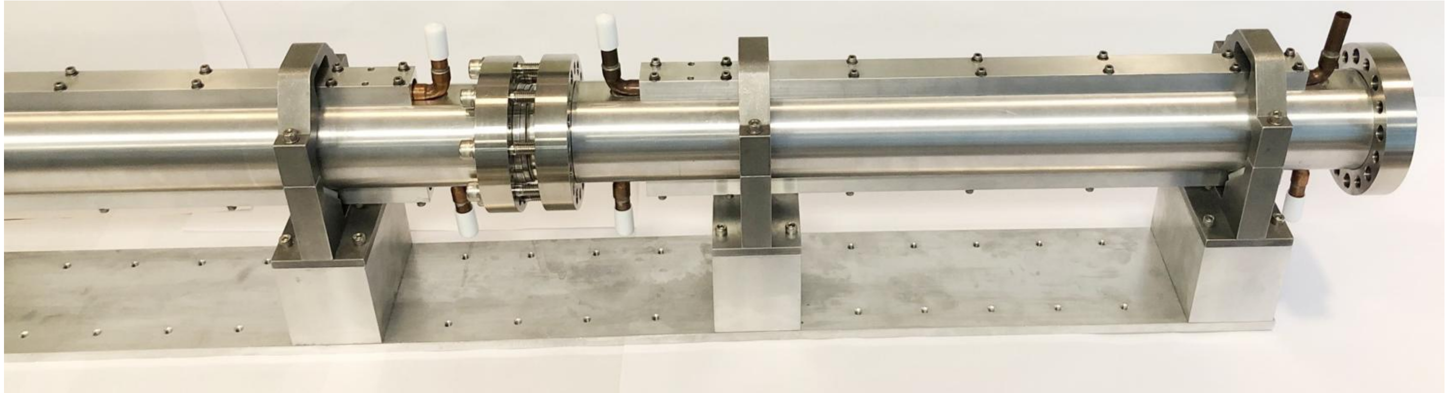

A prototype electron cyclotron transmission line assembly. Photo: US ITER

Linearly Polarized (LP) modes in corrugated WG

- Since the radiated rf-power from the gyrotron is linearly polarized, the excited modes in a corrugated WG are also linearly polarized, LP_{mn}

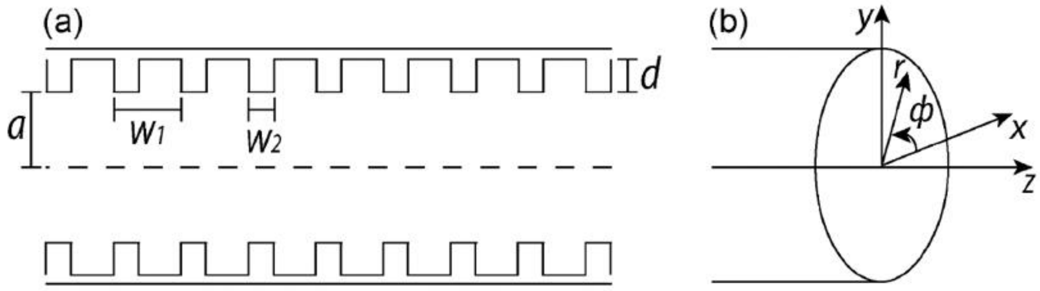

Fig. 1. (a) Cylindrical circumferentially corrugated waveguide with a radius of a. The corrugations are defined by w_1, w_2, and d. For low-loss characteristics, the corrugation depth is $d = \lambda/4$. (b) Illustration of the variables in the cylindrical geometry.

$$Z_z = \infty, \text{ since } kd = \pi/2$$

$$Z_z = \frac{E_z(r=a)}{H_\phi(r=a)} = Z_0 \tan(kd) \quad (1)$$

is the wavenumber and Z_0 is defined by the corrugation

$$Z_0 = -j\frac{w_1 - w_2}{w_1}\sqrt{\frac{\mu_0}{\varepsilon_0}} \quad (2)$$

E. J. Kowalski et al., Linearly Polarized Modes of a Corrugated Metallic Waveguide, IEEE-TMTT, **58** (2010)

Linearly Polarized (LP) modes in corrugated WG

$$E_{y,mn}(r,\phi) = AJ_m\left(\frac{X_{mn}r}{a}\right)\begin{Bmatrix}\cos(m\phi)\\ \sin(m\phi)\end{Bmatrix}, \quad (8)$$

$$H_{x,mn}(r,\phi) = \frac{-Ak_z}{\omega\mu_0}J_m\left(\frac{X_{mn}r}{a}\right)\begin{Bmatrix}\cos(m\phi)\\ \sin(m\phi)\end{Bmatrix} \quad (9)$$

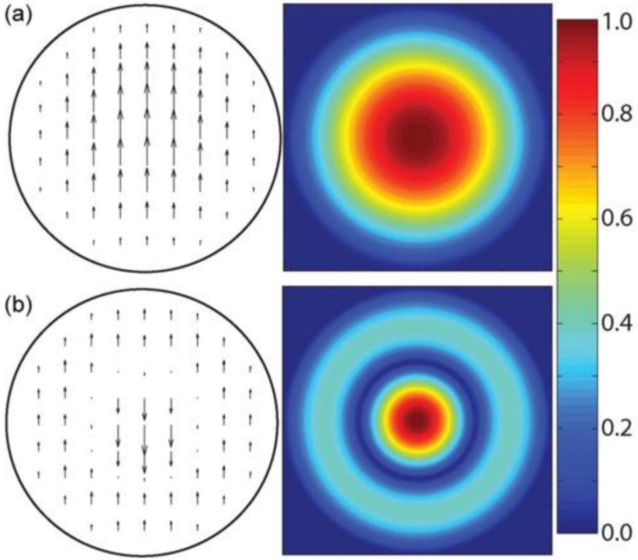

Fig. 2. Field vector and magnitude plots for: (a) LP_{01}/HE_{11} and (b) LP_{02}/HE_{12}. (Amplitudes are normalized.)

Swiss Plasma Center

E. J. Kowalski et al., Linearly Polarized Modes of a Corrugated Metallic Waveguide, IEEE-TMTT, **58** (2010)

Linearly Polarized (LP) modes in corrugated WG [1]

TABLE I
SELECT LP MODES WITH CORRESPONDING DEGENERATE MODES

Mode	X_{mn}	Degenerate modes
LP_{01}	2.405	HE_{11}
$LP_{11}^{(o)}$	3.832	TE_{01}, HE_{21}
$LP_{11}^{(e)}$	3.832	TM_{02}, HE_{21}
LP_{21}	5.136	HE_{31}, EH_{12}
LP_{02}	5.520	HE_{12}
LP_{31}	6.380	HE_{41}, EH_{22}
$LP_{12}^{(o)}$	7.016	TE_{02}, HE_{22}
$LP_{12}^{(e)}$	7.016	TM_{03}, HE_{22}
LP_{22}	8.417	HE_{32}, EH_{13}
LP_{03}	8.653	HE_{13}
LP_{32}	9.761	HE_{42}, EH_{23}
$LP_{13}^{(o)}$	10.17	TE_{03}, HE_{23}
$LP_{13}^{(e)}$	10.17	TM_{04}, HE_{23}

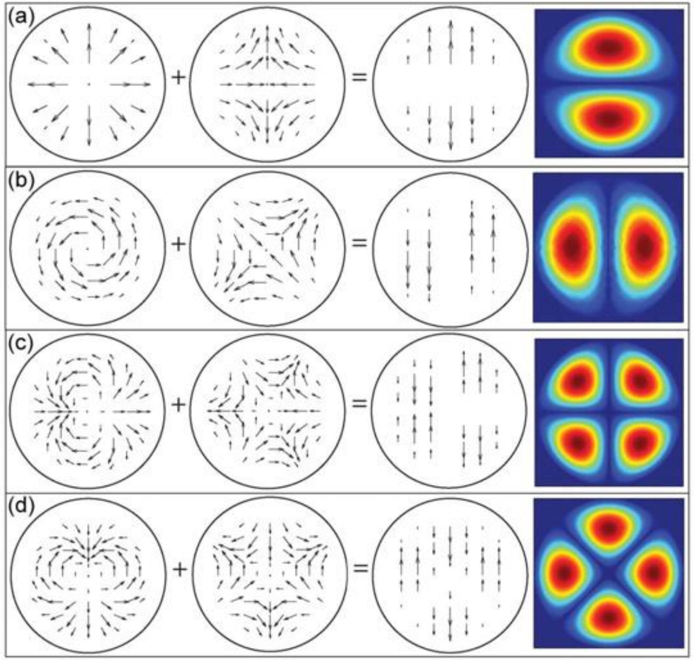

Fig. 3. Field vector plots demonstrating the construction of LP modes from TE, TM, and HE modes. The added modes have identical propagation constants. (a) $TM_{02} + HE_{21}$ rotated 45° $= LP_{11}^{(e)}$. (b) $-TE_{01} + HE_{21} = LP_{11}^{(o)}$. (c) EH_{12} rotated $-90°$ + HE_{31} rotated $-90° = LP_{21}^{(e)}$. (d) EH_{12} rotated $180° + HE_{31} = LP_{21}^{(o)}$.

Swiss Plasma Center

E. J. Kowalski et al., Linearly Polarized Modes of a Corrugated Metallic Waveguide, IEEE-TMTT, **58** (2010)

Losses in corrugated WG

Nucl. Fusion **58** (2018) 106041

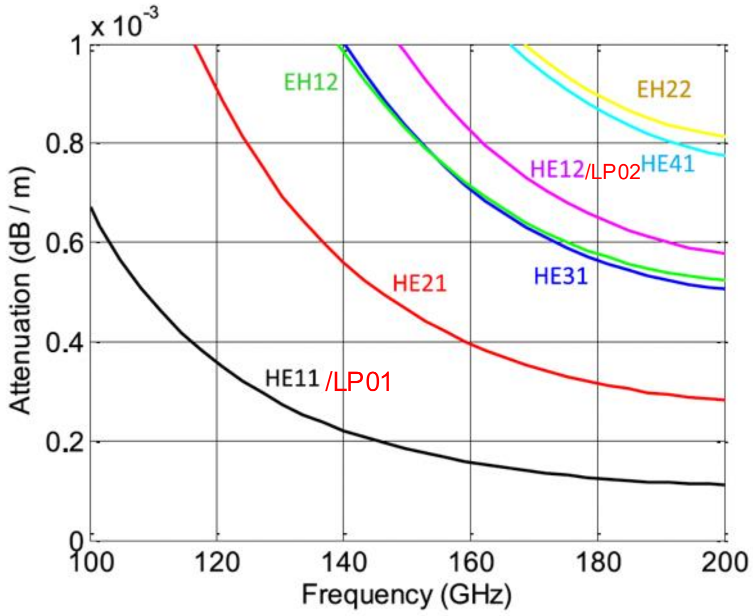

Figure 2. Attenuation of corrugated waveguide.

- 63.5 mm-diameter WG
- Material: 6061-T6 aluminum

Attenuation, α, defined as:

$$P(z) = P_0 \, Exp(-2 \, \alpha \, z)$$

$$\alpha[Np/m] = 0.1151 \, \alpha[dB/m]$$

Y. Oda et al, Nucl. Fusion, 58, 106041

Waveguide, Transmission line, ITER

Falcon Test facility, SPC-EPFL / F4E

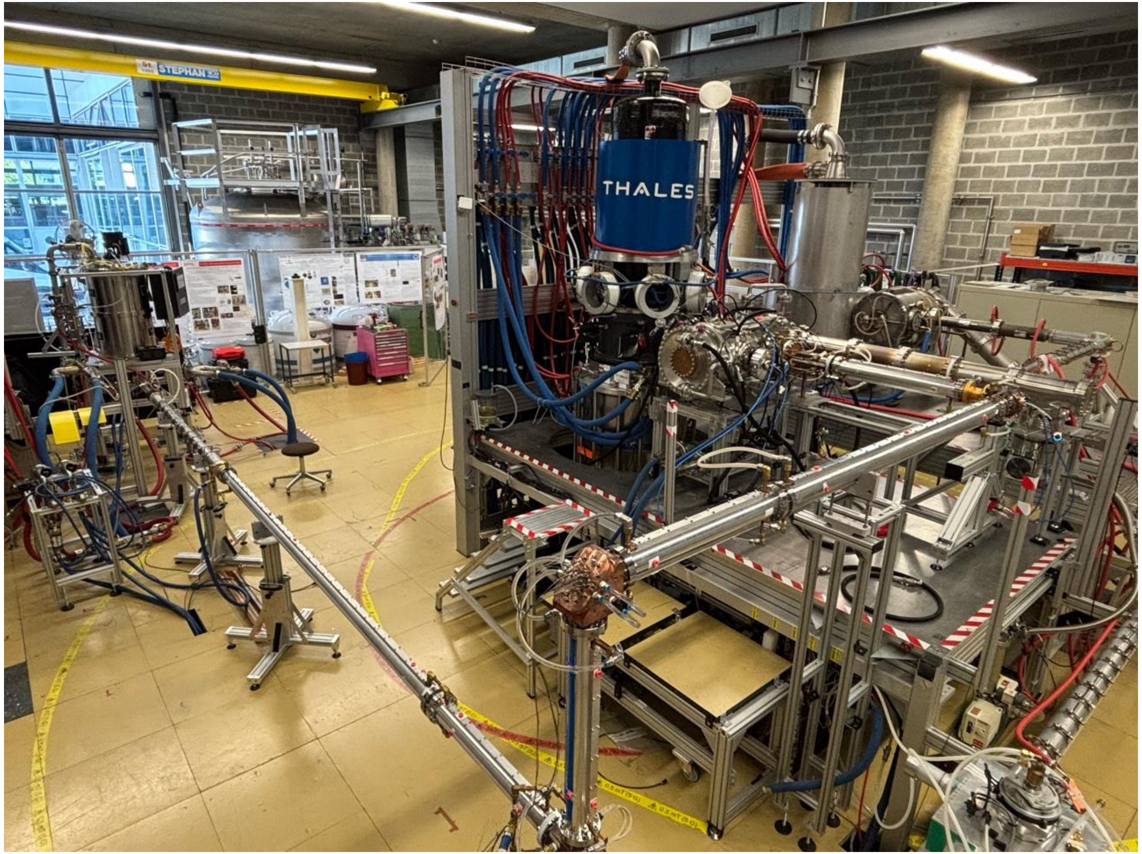

EPFL

WG-component characterization on FALCON

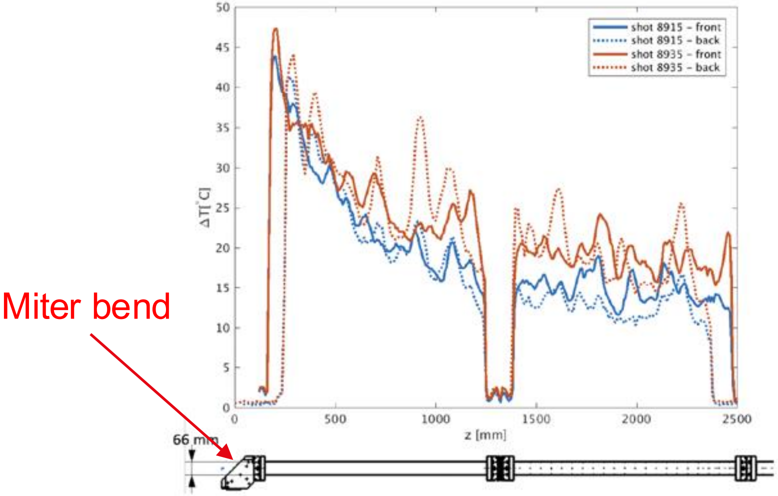

Figure 5. The change in the axial temperature profiles for the original (8915) and misaligned shots (8935) shown in Fig. 4 for both the front (solid) and back (dashed) side. SS WGs show the change in the TL heating pattern when the MOU mirror is misaligned. The relatively high thermal mass coupling between the waveguides appears as a notch centered at ≈1300mm, and at each end. (N.B. The drop in ΔT at each end of the "back" side, shifted with respect to the front side, is due to the size of the reflector - the back is no longer visible to the camera at the extremes.) A sketch of the miter bend and stainless steel waveguides with couplings is shown below the graph.

Swiss Plasma Center

T. Goodman et al, High power mm-wave loss measurements of ITER ex-vessel waveguide components at the FALCON test facility at the Swiss Plasma Center, https://doi.org/10.1051/epjconf/202327704010

Mode purity and losses in corrugated WG

Table 2. Measured mode content at long TL output.

	170 GHz (%)	137 GHz (%)	104 GHz (%)
HE_{11}	93.1	92.5	94.0
HE_{12}	1.1	1.9	0.9
$TE_{01} + HE_{21}$	0.6	0.5	0.9
$TM_{02} + HE_{21}$	1.3	1.7	0.3
$TE_{02} + HE_{22}$	0.3	0.9	0.1
$TM_{03} + HE_{22}$	0.9	0.1	<0.1
Total	97.4	97.6	96.3

Table 3. Measured mode content at short TL output.

	170 GHz (%)	137 GHz (%)	104 GHz (%)
HE_{11}	94.4	91.9	92.7
HE_{12}	0.3	1.6	1.5
$TE_{01} + HE_{21}$	1.5	1.6	0.7
$TM_{02} + HE_{21}$	0.2	1.5	0.2
$TE_{02} + HE_{22}$	0.8	0.6	0.1
$TM_{03} + HE_{22}$	0.3	0.1	<0.1
Total	97.4	97.3	95.2

Table 4. Transmission efficiency of TL for multi-frequency operation.

	170 GHz	137 GHz	104 GHz
Gyrotron output power	430 kW	320 kW	260 kW
Transmission power efficiency			
Transmission efficiency at MOU	96.7%	94.2%	90.2%
Transmission efficiency at long TL	93.8%	95.1%	93.7%
Total transmission efficiency (MOU + long TL)	90.7%	89.6%	84.5%
Mode purity			
HE_{11} mode purity at MOU output	94.4%	92.6%	92.7%
HE_{11} mode purity at Long TL end	93.1%	92.5%	94.0%

Y. Oda et al, Nucl. Fusion, 58, 106041

Polarization of EM-wave

- More generally: tilt of the ellipse $\boldsymbol{\alpha}$ (relative to the x axis)
- The wave polarization is in general elliptical
  - Particular cases
    - $\beta = 0 \Rightarrow$ linear polarization
    - $\beta = \frac{\pi}{4} \Rightarrow$ circular polarization

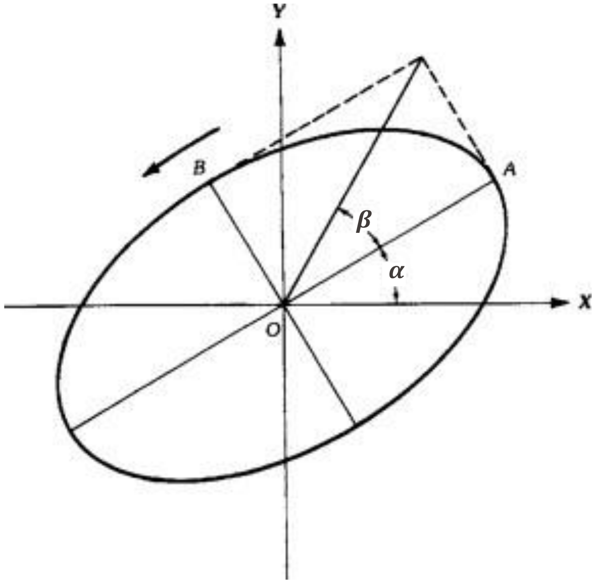

For ECRH and ECCD experiments, one needs to control the angles α and β

Polarizers

- Universal polarizers composed by two metallic mirrors with grating on the surface, allowing the control of the polarization
- Polarizer rotator
- Elliptical polarizer
- Use of mirrors with grating

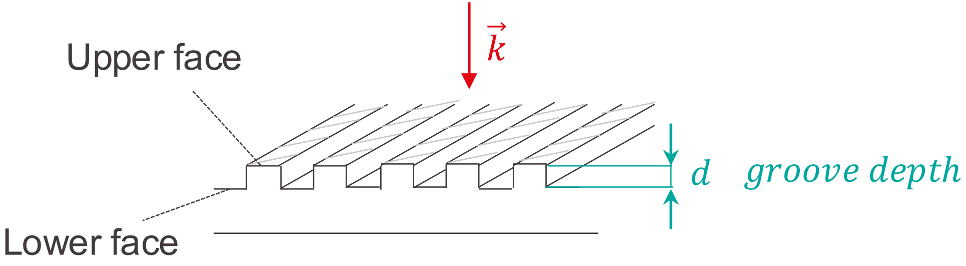

Example, GA design

Mirror actuator for real-time control of polarization

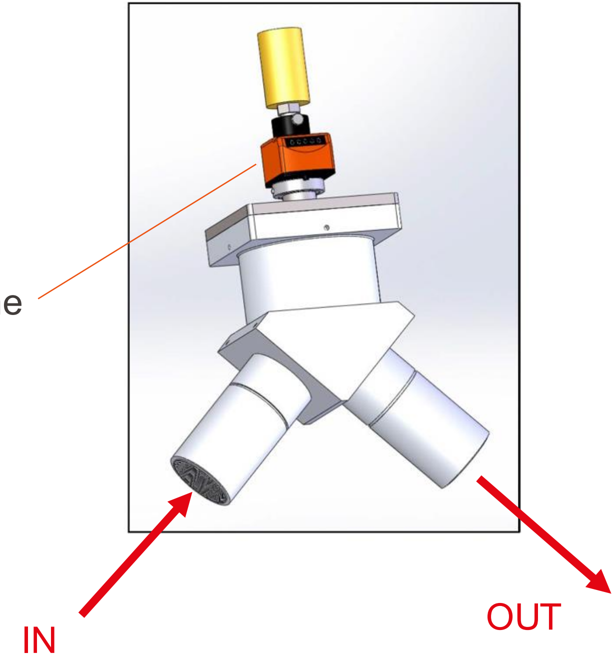

Transmission line components

Diamond Window Unit

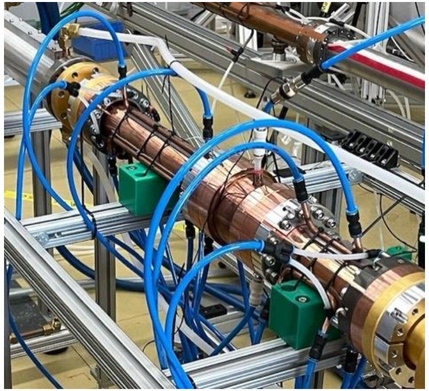

Switch

GCC

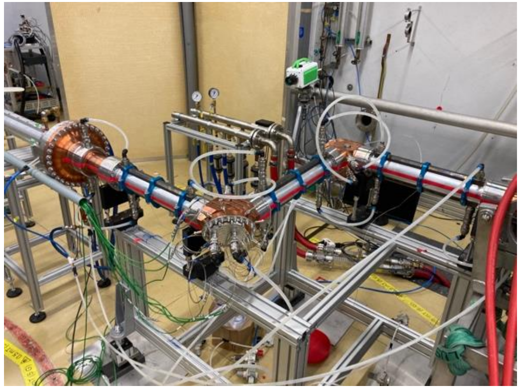

Isolation valve

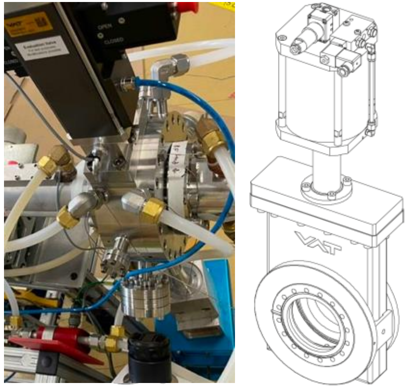

Transmission line components, tests

- Each of these components need to be tested in realistic operation conditions (1MW, CW)
  - Power loss
  - Effect on mode purity
  - Thermal testing
    - In case of ideal operation
    - With some misalignment
  - Vacuum qualification

Calorimetric measurements

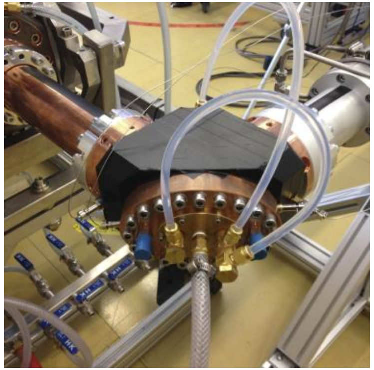

Beam measurement

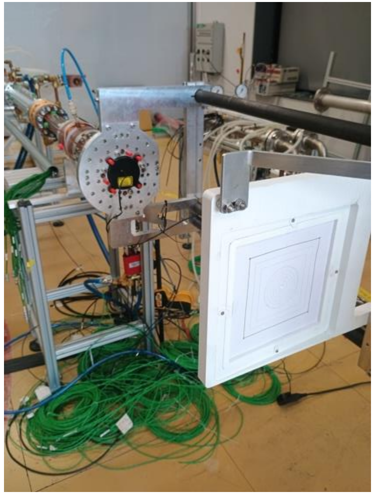

Infrared measurements

ITER external heating systems

Outline

- 1. Sources
- 2. Transmission and component
- 3. Launchers

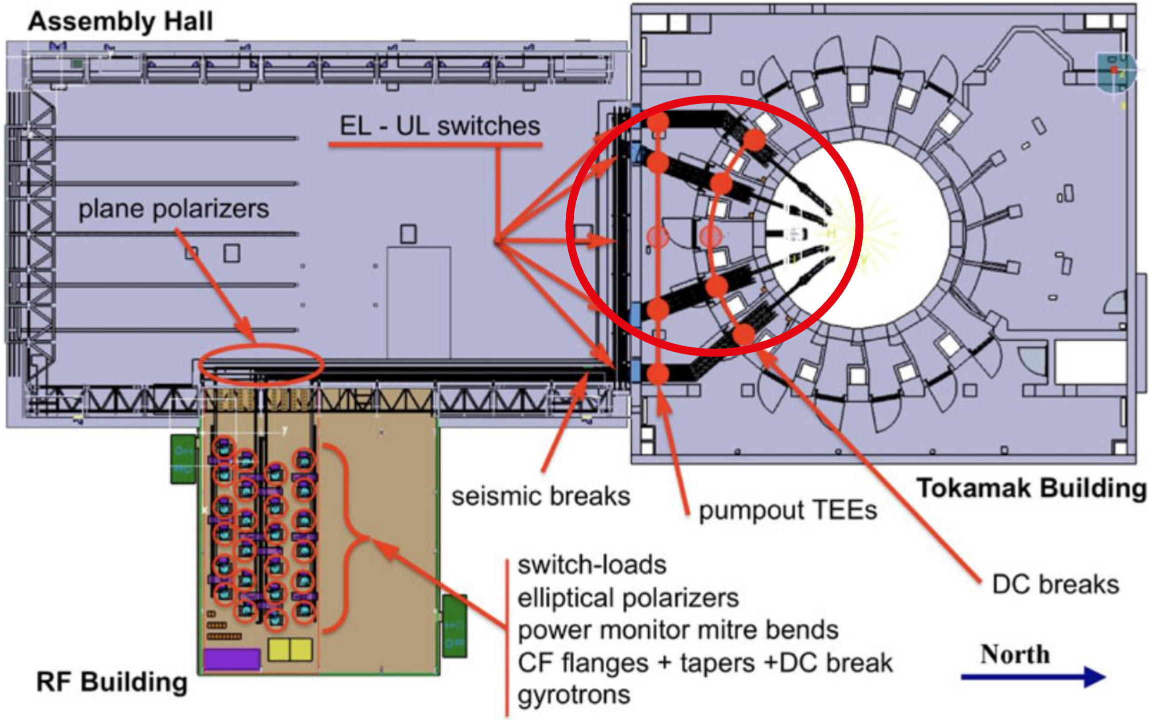

F. Gandini, Fusion Science and Technology (2010)

Launchers for ITER

- 4 Upper Launchers (4 x 8 entries)
  - Stabilization of the plasma: suppression of NTMs, sawtooth control
  - Localized ECCD
- 1 Equatorial Launcher (24 entries)
  - Central heating
  - ECCD
  - Assisting plasma startup

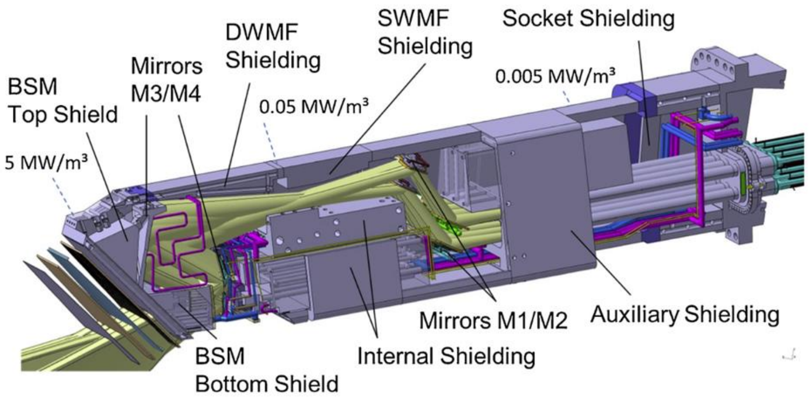

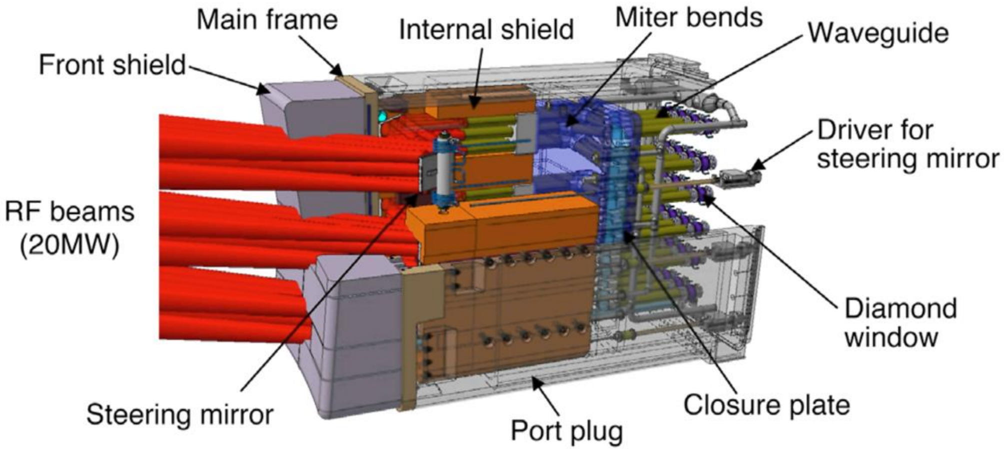

Mock-up tests

UL mock-up tests at FALCON

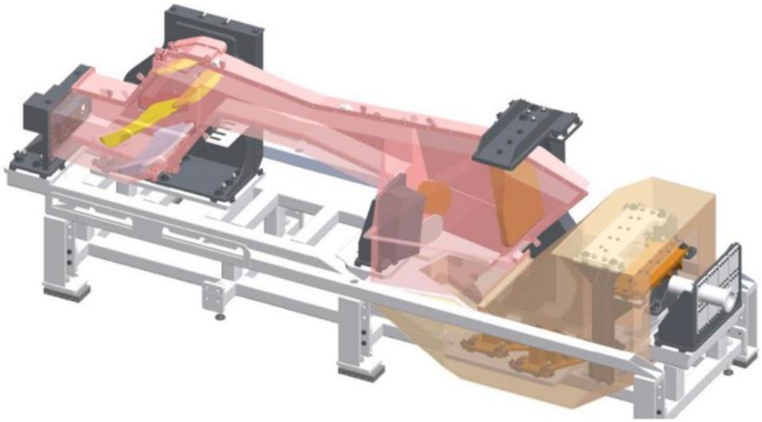

F. Braunmüller, et al., IAEA FEC 2025

EL mock-up tests (JAEA, ITER JADA)

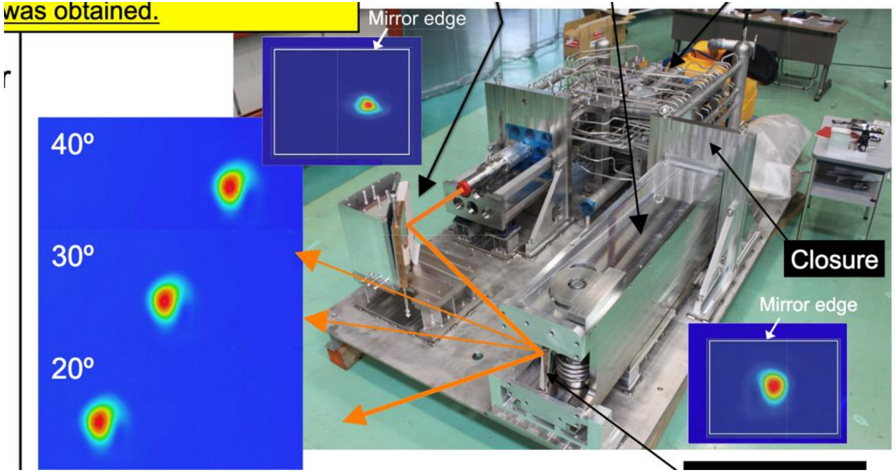

K.Takahashi, et al., IAEA FEC 2013

Mock-up tests

- As the TL components, the launchers need to be tested:
  - Power loss
  - Effect on mode purity
  - Thermal testing
    - In case of ideal operation
    - With some misalignment
  - Vacuum qualification
  - Neutronics

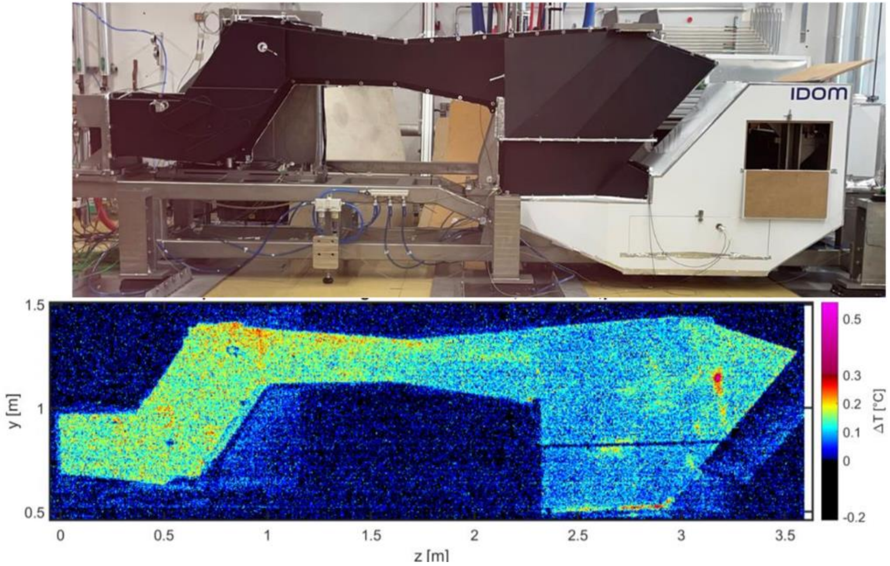

F. Braunmüller, et al., IAEA FEC 2025

Conclusion

- The EC technology for ITER is mature and many components are ready for deployment
- Further improvement remains possible, in particular for the gyrotrons
  - Higher efficiency
  - Increased reliability
- Looking beyond ITER
  - Challenging development for gyrotrons
    - Higher frequency/power
    - Higher efficiency
    - Higher reliability
    - Industrial-scale production
- Further R&D is essential to meet the demands of future fusion power plants

Thank you for your attention